Pulsed and time-resolved optically stimulated luminescence of natural minerals – A review

Riedesel, Svenja; Ankjærgaard, Christina

Published in:
Radiation Measurements

Link to article, DOI:
10.1016/j.radmeas.2025.107596

Publication date:
2026

Document Version
Publisher's PDF, also known as Version of record

Radiation Measurements 191 (2026) 107596

Contents lists available at ScienceDirect

Radiation Measurements

journal homepage: www.elsevier.com/locate/radmeas

Pulsed and time-resolved optically stimulated luminescence of natural minerals – A review

Svenja Riedesel [a,b,*], Christina Ankjærgaard [c]

[a] Institute of Geography, University of Cologne, Cologne, Germany
[b] Luminescence Physics and Technologies, Department of Physics, Technical University of Denmark, Lyngby, Roskilde, Denmark
[c] Dosimetry, Department of Health Technologies, Technical University of Denmark, Lyngby, Roskilde, Denmark

ARTICLE INFO

Keywords:
Time-resolved luminescence
Pulsed stimulation
Lifetime
Thermal quenching

ABSTRACT

Time-resolved luminescence measurements provide a powerful means of investigating luminescence processes across timescales, ranging from picoseconds to seconds. These measurements are typically enabled by pulsed stimulation, where light pulses of fixed durations are applied to a sample. Luminescence can then be recorded both during and after the pulsed light stimulation, allowing discrimination between stimulation and emission, as well as isolation of luminescence components with different lifetimes.

Quartz and feldspar minerals are the two natural minerals most commonly used in luminescence studies. Time-resolved luminescence of feldspars has been investigated since the early 1990s, while quartz time-resolved signals has come into focus since around 2000. Over the past three decades, the extensive research into time-resolved and pulsed luminescence properties of these two minerals has provided insights into the lifetime of recombination and relaxation processes of various emissions in these minerals. These differences in the luminescence decay of quartz and feldspar offers a practical solution for discriminating their luminescence.

This review is aimed at researchers specialising in the field of luminescence dating, who embark on their first pulsed and time-resolved luminescence journeys. It provides practical information on measurement techniques for conducting time-resolved luminescence measurements and presents an overview of research findings, accumulated over the past 3.5 decades highlighting both the fundamental processes revealed and the applications enabled by these methods.

1. Introduction

1.1. Content and aim of this review

This review, which focuses on pulsed and time-resolved optically stimulated luminescence (OSL) of natural minerals, is primarily targeted at researchers specialising in the field of luminescence dating. It also provides technical information for those new to the concepts and practical aspects of time-resolved luminescence measurements of any luminescent material. The focus of the review is to introduce the reader to possibilities when performing time-resolved luminescence measurements and to highlight key features of time-resolved luminescence of the natural minerals most commonly used in luminescence dating applications: quartz and feldspar.

The review outlines the general principles of pulsed stimulation and time-resolved luminescence measurements, emphasizing the differences between the two most commonly used instrumentation methods. It introduces the underlying physical concepts of pulsed and time-resolved luminescence through their application to quartz and feldspar minerals. Our application-based approach aims to clarify the processes behind the luminescence of natural materials and, we hope, will inspire readers to embark on their own experimental investigations.

By reading this review, you will find a detailed answer to these and many more questions: What capabilities does time-resolved luminescence offer, and why might this technique prove essential for advancing your research?

1.2. A brief overview of pulsed stimulation and time-resolved measurements

Optically stimulated luminescence (OSL) dating of natural minerals in geochronology typically employs continuous wave (CW) stimulation.

* Corresponding author. Institute of Geography, University of Cologne, Cologne, Germany
E-mail address: svenja.riedesel@uni-koeln.de (S. Riedesel).

https://doi.org/10.1016/j.radmeas.2025.107596
Received 10 September 2025; Received in revised form 2 December 2025; Accepted 15 December 2025
Available online 16 December 2025

In this method, light emitting diodes (LEDs) or lasers, are used to stimulate trapped charge in the crystal lattice, causing the eviction of charge (mostly trapped electrons) from defects within the crystal. In contrast, pulsed stimulation is based on administering short (on the pico-, micro- or millisecond timescale) light pulses to induce the release of trapped charges. This method enables the measurement of emitted luminescence both during the stimulation pulse and in the intervals when the light is turned off. Such separation of stimulation and detection phases enhances the signal-to-noise ratio by allowing asynchronous luminescence detection, even for emissions with wavelengths close to that of the stimulating light. Moreover, when combined with time-resolved luminescence techniques, pulsed stimulation permits precise delineation of the timescales associated with different luminescence processes, such as electron-hole recombination or (re-)trapping.

Fig. 1 illustrates the differences between CW and pulsed stimulation and the respective luminescence signals obtained from these two different methods of stimulation. CW stimulation (Fig. 1A) releases trapped charge, which after recombining at a hole centre, results in the detection of a decaying luminescence signal, with the intensity decreasing over time, until a stable (and low) background level is reached (Fig. 1B).

Fig. 1C illustrates the different light pulses administered to a sample. When performing pulsed luminescence measurements, multiple short light pulses of fixed times are emitted over a longer period of time. The duration of the light pulse is referred to as *on-time*, whilst the intervals between each light pulse are termed *off-time*. The duration of the on-time is referred to as pulse width. Note: Except for q-switch (a special technique, which allows fast switching of the laser) laser pulses, the temporal response of the stimulation light source to the electrical switching needs to be taken into account. The sequence of multiple on- and off-times over a longer duration is referred to as the stimulation period. Below we explain further definitions of the terminology used in this review.

Two different signals can be measured when performing pulsed stimulation (cf. Fig. 1C–G).

1. Time-resolved signal: Time-resolved luminescence signals are composed of two distinct components: the on-time signal and the off-time signal (cf. Fig. 1E and F). During the on-time period, a brief light pulse stimulates the sample, thereby releasing trapped charge carriers. This release may result in either (re)trapping or recombination, both of which can emit photons; however, the number of emitted photons is typically sufficiently low to be individually detected by the instrument (cf. Fig. 1E and F). In contrast, during the off-time period, no additional light is provided, so no new charge is released from the traps. Nevertheless, charge carriers excited during the on-time, which reached the excited state of a defect, may still relax to the defect's ground state. If an excited electron is located

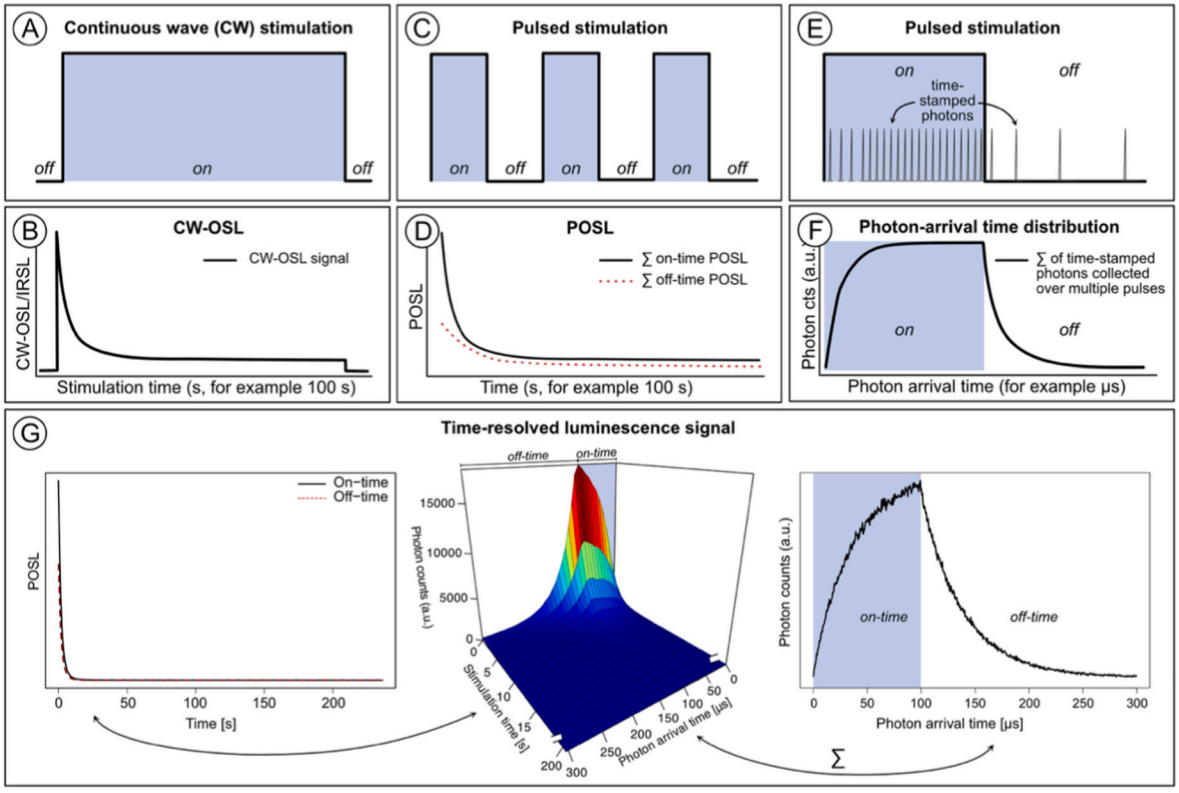

Fig. 1. Pulsed and time-resolved luminescence measurements are complex and consist of different components. This figure schematically outlines these components and illustrates the corresponding luminescence signals measured. (A) During a standard continuous wave stimulation measurement, the stimulation light is kept at a constant power over the stimulation period. Short off-times (or dead channels) at the beginning and end of each measurement allow for the background counts to be observed. (B) The resulting CW-OSL curve, with a decaying luminescence signal over the stimulation period. (C) During pulsed stimulation the stimulation light source is pulsed on and off for set amounts of time. (D) A luminescence decay curve can be obtained for the on- and off-time respectively, when the respective luminescence is summed. If the respective on-time signal should have the same stimulation length as the CW-OSL signal, then the stimulation length of the entire pulsed signal needs to be adjusted accordingly, e.g. if the on- and off-time ratio is 1, then the measurement will take twice as long, compared to a CW-measurement, because 50 % of the measurement time is spend recording the off-time signal. (E) During each individual pulse photons are emitted, and the time of their detection is measured, allowing the development of a cumulative temporal spectrum of the emission characteristics to be measured. (F) After many thousands of pulses a photon-arrival time distribution can be created. (G) Here an illustrative example of a quartz time-resolved blue-LED stimulated luminescence signal is displayed (3D plot in the middle). For the respective on- and off-time the pulsed OSL curves are shown on the left and the sum of photons recorded versus their arrival time on the right. (For interpretation of the references to colour in this figure legend, the reader is referred to the Web version of this article.)

within a defect with an allowed transition, the probability of radiative recombination remains constant over time. This leads to first-order kinetics, characterised by an exponential decay in luminescence intensity during the off-time. The decay reflects the intrinsic lifetime of the excited state, and its lower intensity compared to the on-time signal is due to fewer excited electrons available for recombination once stimulation ends. The off-time luminescence thus offers valuable insights into the kinetics and timing of relaxation processes, such as electron-hole recombination and transitions from excited to ground states.

2. POSL curve - pulsed optical stimulation curve: By summing the luminescence emitted during successive on-time pulses, a curve is produced that closely resembles that obtained using CW stimulation (Fig. 1D). This allows pulsed stimulation to be used in standard luminescence experiments, such as generating dose-response curves. The resulting OSL decay curve can represent the entire signal or be derived from the on-time or off-time components separately (Fig. 1D). When luminescence is recorded and summed during a specific part of the measurement, mostly during the off-time, it is referred to as a gated signal. Setting the gating in pulsed measurements ensures the recorded interval is well-defined and summed automatically. In section 5 we provide examples demonstrating the advantages of pulsed stimulation and gated signals over conventional CW signals in luminescence dating applications. (i.e. Denby et al., 2006; Ankjærgaard et al., 2010; Tsukamoto et al., 2017).

In this review we use the following terminology when describing time-resolved luminescence measurements:

On-time refers to the duration of each stimulation pulse, which is adjustable based on the luminescence behaviour of the studied sample and the properties of the stimulation light source. Typically, the duration of these pulses ranges from ps to μs. On-time is also referred to as pulse width in the literature (e.g. Tsukamoto et al., 2006; Chithambo, 2007a,b).

Off-time describes the duration of the pause between two consecutive stimulation pulses and where the decaying part of the luminescence signal is detected. The off-time can be adjusted and is usually in the same order of time as the on-time. This is sometimes also denoted as the *sweep*, see below.*Photon arrival time* refers to the time interval between the start of a stimulation pulse and the emission of a photon. Technically, this is also influenced by the measurement equipment, specifically the time delay between photon emission and detection by the photomultiplier tube (PMT) or the photon counter.

Stimulation time refers to the duration from the start of the optical stimulation to the conclusion of the measurement. It encompasses multiple on- and off-time intervals and is typically in the order of seconds.

Further technical terms used elsewhere in the time-resolved luminescence literature include:

Period: The term *period* is sometimes used to describe the time between the start of two excitations, which is also the sum of one on- and off-time cycle (e.g. Chithambo, 2011; Knoll, 2010).

Dynamic range: The *dynamic range* is the ratio between maximum and minimum detectable signal intensities. These limits are usually defined by the instrumental setup, where the upper limit is given by the maximum measurement capacity of the instrument, before signal saturation is reached. The lower limit is dependent on the background noise (e.g. Tosi et al., 2011).

Sweep: The term sweep is also used to describe the measurement window after the stimulation pulse, which in this paper is the off-time (Knoll, 2010).

In most studies, the main purpose of performing time-resolved luminescence measurements is to determine the lifetime of the signal recorded during these measurements. During the on-time, light stimulation of the samples causes the excitation of charge from the ground state of a defect to the excited state, from which it relaxes back to the ground state, often under the emission of photons. Once the stimulation light source is switched off, no new ground-to-excited state excitation will take place but charge already excited to the excited state of the defect will still relax to the ground state. This process can be monitored during the off-time, if the relaxation process is associated with the emission of photons. In these cases, the relaxation is referred to as radiative transition. Fitting the during the off-time recorded luminescence signal provides a means of quantifying the time needed for this radiative relaxation. The determined time is referred to as lifetime, and is commonly denoted as τ.

Lifetimes are controlled by the type of defect in which radiative relaxation occurs, and they can vary considerably. For different materials and defects, lifetimes span a wide range, from fast lifetimes on the nanosecond (ns) timescale to slower lifetimes associated with phosphorescence decay, which can range from milliseconds (ms) to seconds (s). Examples of these diverse lifetimes, along with the defects responsible for them, are presented in sections 3 and 4 of this review.

2. Instrumentation and measurement conditions for time-resolved measurements

This section outlines the key considerations for configuring time-resolved luminescence experiments and describes the instrumentation and measurement conditions necessary to achieve specific research objectives. Which type of instrumentation is best suited for a given measurement? We explore this by discussing different aspects of instrumentation, including the two primary techniques: multichannel scaling and time-correlated single-photon counting (TCSPC). Multichannel scaling records photon arrival times in predefined time bins, yielding a histogram-based decay curve with relatively compact data sets. In contrast, TCSPC time-tags each photon relative to the stimulation pulse, offering flexible post-processing and enhanced temporal resolution, albeit with larger data volumes. Each method presents distinct advantages and limitations, and the choice between them depends on the experimental requirements and the characteristics of the luminescent material under investigation.

2.1. How to stimulate the sample during time-resolved measurements?

Time-resolved luminescence measurements utilise pulsed optical stimulation to capture the luminescence signal both during the on-time and during the off-time. Often the off-time signal is of greater interest, because it will inform on the excited state lifetime of the defect probed in the specific measurement (e.g. Clark et al., 1997; Riedesel et al., 2023). Dependent on the excited state lifetime measured, the type of stimulation light source should be chosen. The faster the decay (i.e. shorter lifetime in the excited state) the shorter the stimulation pulse needs to be to optimally reduce its overlap with the emitted luminescence.

The relationship between the on-time (or pulse width) t_1, the luminescence lifetime $\tau = 1/\lambda$, and the fraction of luminescence detected after the end of the stimulation pulse is described following Chithambo (2007a) using equation (1):

$$f = \frac{1}{\lambda t_1}[1 - exp(-\lambda t_1)], \quad [1]$$

Where $f = L_{off}/L_T$ is the fraction of the total luminescence L_T of the time-resolved luminescence signal, and L_{off} the luminescence emitted after the stimulation pulse. Equation (1) demonstrates that the amount of luminescence emitted after the stimulation pulse increases as the length of the on-time (or pulse width) decreases relative to the lifetime of the luminescence signal. Thus, to maximise the measurable off-time luminescence (L_{off}), the stimulation pulse width should be shorter than the luminescence lifetime (cf. Chithambo, 2007a).

The narrowest pulses are typically obtained with Q-switched laser sources, but the switching speeds of laser diodes and LEDs are being

progressively reduced. The switch-off time of the stimulation light source defines the lower detection limit for the lifetimes under investigation. For example, if the chosen stimulation light source has a switch-off time of 0.5 μs, lifetimes shorter than 0.5 μs are difficult to resolve, if they exist. This is because the light pulse and the short lifetimes may overlap, making it impossible to distinguish them using traditional exponential fitting methods. To address overlap in exponentially decaying signals, deconvolution techniques, such as those involving the inverse Laplace transform and regularisation (e.g. Talele and King, 2021), can be employed. These methods provide both theoretical and practical means to separate overlapping decay components by extracting their individual decay constants. It is crucial to ensure that the available light sources have a sufficiently fast switch-off time for the required analysis, especially when dealing with overlapping decay signals.

Often lasers offer advantages over LEDs due to their faster switch-off time and higher power. Dependent on the size of the sample, a focused laser beam, however, might be inappropriate for stimulating sample areas larger than the focused beam. Here inserting a diffuser, specific equipment, which distributes light evenly across a surface, will help in increasing the stimulated samples area, whilst keeping the advantage of the fast switch-off time.

Prior to the experiments it is important to measure how fast the stimulation light source will switch off. To investigate this, the actual LED or laser light emission needs to be measured. During this, it is important to take care not to damage the detection unit.

To be able to measure the switch-off time of the LEDs without damaging the detector, a filter needs to be inserted, which will significantly reduce the amount of stimulation light being detected, by still having sufficient signal remaining for determining the switch-off time of the LEDs. Ideally, one would like the filter to have a broad transmission range, but a high optical density.

The optical density describes how much of the incoming light is blocked by the filter. The higher the optical density (OD) the less light will be transmitted by the filter. The relative transmission [%] of a filter is calculated following equation (2):

$$Transmission\ [\%] = 10^{-OD*100} \quad [2]$$

Which results in equation (3):

$$Optical\ density = -log\frac{Transmission}{100} \quad [3]$$

Filters termed neutral density filters have such properties. They are designed to reduce the transmission evenly across a defined range of the wavelength spectrum and can thus be used to reduce the transmission of the stimulation light by a certain percentage, dependent on the filter's OD. Once all the required equipment is in place, it is possible to perform a time-resolved measurement of the LED emission and detecting its signal through the chosen neutral density filter.

Fig. 2 shows measurements of the switching characteristics of blue, green and infrared LEDs measured using an oscilloscope. Similar results would have been achieved by using the PMT fitted with a neutral density filter.

Excitation and emission spectroscopy on materials such as quartz and feldspar provide essential guidance on selecting appropriate stimulation and emission wavelengths (e.g. Hütt et al., 1988; Bøtter-Jensen et al., 1994). Often, the stimulation and emission wavelengths are well separated — for instance, quartz OSL measurements typically use blue or green light for stimulation with UV emission (~340 nm), while feldspar studies often employ IR stimulation (~850 nm) with blue emission (~410 nm). However, pulsed stimulation enables discriminating between excitation and emission signals even when their wavelengths are closely spaced. This capability is particularly important in detecting the infrared photoluminescence (IRPL) of feldspars, where the stimulation (830 nm) and emission (880 nm) windows are in close proximity. In such cases, the IRPL signal is measured during the off-time of the stimulation laser diode, thereby reducing interference (e.g. Kook et al., 2018; Kumar et al., 2021). Riedesel et al. (2023) demonstrated that breakthrough from the 830 nm laser is clearly visible during $IRPL_{880}$ measurements, with most of the laser signal decaying within the first 0.1 μs of the off-time. Although this method offers an advantage, it should be noted that closely spaced excitation and emission windows can introduce additional complications. Pulsed laser stimulation at short wavelengths may induce secondary fluorescence in the glass detection filters, and if the lifetime of this secondary fluorescence extends into the detection window where its spectral range overlaps with that of the target emission, it may compromise the measurement. This issue is especially pronounced with high-power laser pulses that produce significant scattered light, underscoring the importance of careful optical system design.

2.2. How to count the photons during time-resolved measurement?

Special equipment is necessary to record the time-resolved luminescence signal. Mostly two different types of equipment are used for this purpose: a multichannel scaler or time-correlated photon counting (TCSPC).

A **multichannel scaler** records the time distribution of photon arrivals following each stimulation pulse, with the time bins being adjustable based on the instrument's capabilities. The bin width is typically selected prior to the measurement. The scaler enables the collection of specific photon emission events within predefined time bins and the construction of a histogram depicting the distribution of photon arrival times. However, limitations related to the bit counting capacity of the counter may arise. If the bit depth is insufficient, the counter may fail to capture rapidly arriving photons or adequately detect individual photons in highly luminescent materials. (cf. Clark et al., 1997).

In contrast, **time-correlated single-photon counting (TCSPC)** records each photon detection with a precise time-stamp relative to the

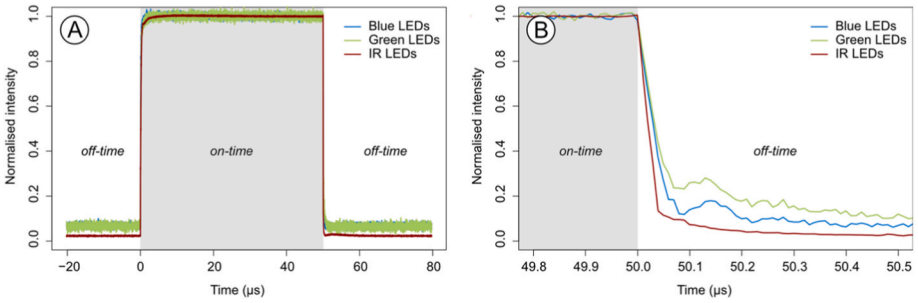

Fig. 2. A) Switch on- and switch off-times for blue, green and IR LEDs. These signals are displayed using an oscilloscope, by prompting the LEDs build into a commercially available luminescence instrument. The total on-time was set to 50 μs. (B) is expanded to the timescale showing the switch-off characteristics of the LEDs. (For interpretation of the references to colour in this figure legend, the reader is referred to the Web version of this article.)

preceding stimulation pulse. By accumulating these time-tagged photons, it is possible to create a photon arrival time distribution with customisable bin widths, offering greater flexibility in data post-processing. However, one drawback of TCSPC is the substantial volume of raw data generated, in contrast to the relatively smaller data files produced by multichannel scalers. While multichannel scaling results in less data, it lacks the same level of post-processing versatility provided by TCSPC.

2.3. Time-resolved luminescence of natural materials

In luminescence dating studies constraining archaeological, geological and geomorphological events and processes, two types of natural minerals are of main interest: quartz (SiO_2) and feldspar ($KAlSi_3O_8$, $NaAlSi_3O_8$ or $CaAl_2Si_2O_8$). Time-resolved measurements of their luminescence have been performed to gain insights into charge recombination and relaxation processes in these minerals (e.g. Clark et al., 1997; Bailiff, 2000; Jain et al., 2015; Riedesel et al., 2023). Furthermore, studies have demonstrated that pulsed stimulation, where time-resolved signals were measured during the off-time of the stimulation pulse, can effectively differentiate the luminescence of these two minerals in mixed samples (Bailiff and Mikhailik, 2003; Denby et al., 2006; Thomsen et al., 2008; Ankjærgaard et al., 2010). A useful tool to reduce the impact of feldspar contamination in natural quartz samples. Fig. 3 shows the differences in quartz and feldspar luminescence signal shapes during the on- and off-time of pulsed stimulation. Research into the luminescence lifetimes of quartz and feldspar have shown early on that the characteristic luminescence lifetimes differ significantly. The luminescence from quartz decays over ~30–~40 μs, while feldspar luminescence can be characterised as a mix of multiple lifetimes, spanning timescales from a few tens of ns to a few μs (cf. Sanderson and Clark, 1994; Clark et al., 1997; Bailiff, 2000). The following sections will introduce time-resolved luminescence of quartz and feldspar, and the application of pulsed stimulation to discriminate between the luminescence emitted by these two minerals.

3. Quartz [SiO_2] time-resolved luminescence

This section investigates the time-resolved luminescence of quartz and the processes involved in its luminescence emission. Key questions that we aim to answer in this section are: Which transitions are measured using time-resolved luminescence? But also, what influences the resulting lifetimes of the luminescence emission? Understanding these are crucial for interpreting the luminescence behaviour of quartz and its applications in areas such as luminescence dating. Quartz (SiO_2) is the most widely used natural dosimeter in luminescence dating, and it is commonly believed that quartz luminescence follows first-order kinetics. These processes have been modelled using the one-electron-trap-one-recombination-centre (OTOR) model (e.g. Chen et al., 1990; McKeever, 1994; based on Randall and Wilkins, 1945), although more

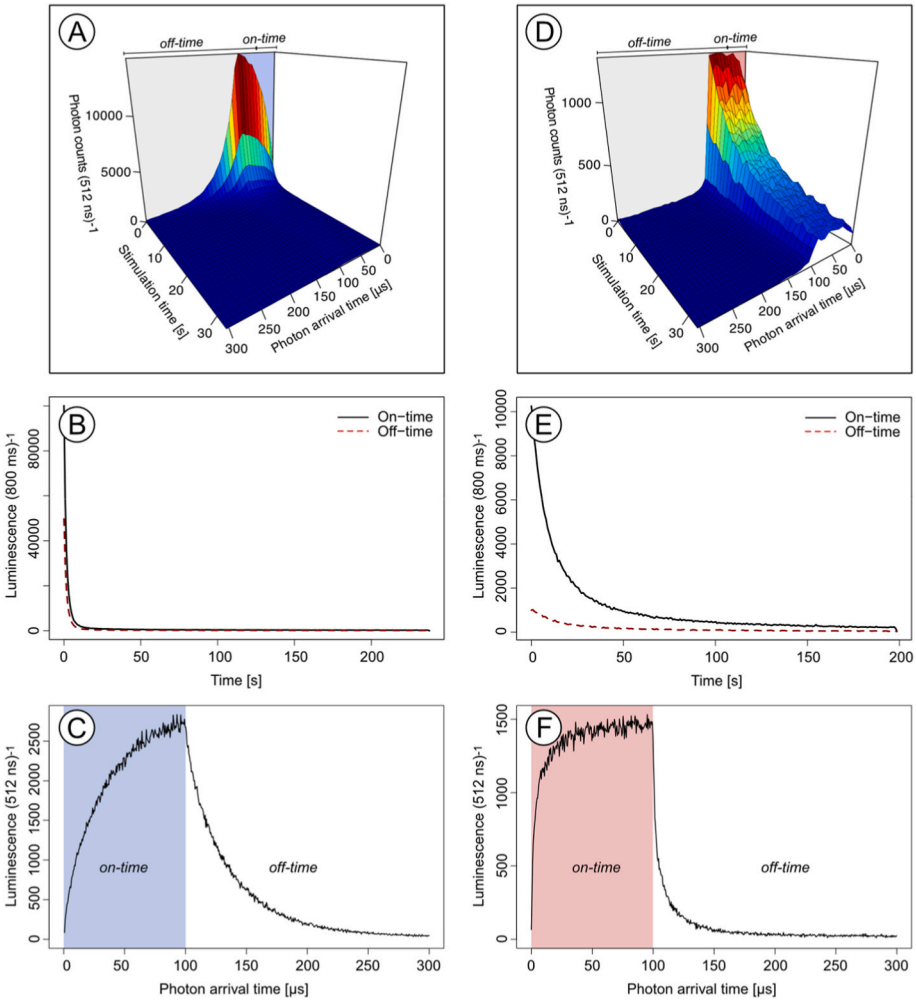

Fig. 3. Examples of time-resolved signals measured for quartz (A to C) and feldspar (D–F). Figures A and D show the three-dimensional plots of time-resolved signals, with only the initial 30 s of the stimulation time shown. The pulsed OSL and IRSL signal integrated over the on- and off-time is shown in B and E. The last two panels (C and F) show the photon arrival time distributions for quartz (C) and feldspar (F), respectively. The respective on-times are highlighted with shaded areas.

complex models exist (e.g. Bailey, 2001). According to the OTOR model, luminescence production in quartz occurs when an electron is excited from its ground state in the electron trap to the conduction band, followed by recombination with a hole at a recombination centre. This is followed by relaxation from the recombination centre's excited state to its ground state. The three key transitions involved in this process are (1) electron eviction, (2) charge transfer through the conduction band, and (3) relaxation from the excited state to the ground state within the recombination centre (see transition B′ to B in Fig. 4A). These transitions are reflected in the lifetimes observed when measuring the quartz optically stimulated luminescence (OSL) time-resolved signal (e.g. Ankjærgaard and Jain, 2010a,b). Among these processes, the latter two are typically viewed as the dominant contributors to luminescence. However, their relative contributions depend on the type of recombination centre probed during the measurements. When the recombination process involves a radiative transition from the excited state to the ground state of the recombination centre, the luminescence lifetime is influenced by the nature of this transition: it will be fast for allowed transitions and slow for (partially) forbidden transitions (e.g. Ankjærgaard and Jain, 2010a,b).

3.1. An overview of lifetimes obtained for quartz luminescence

The first to constrain the lifetime of the quartz OSL signal was Bailiff (2000). He compared the time-resolved luminescence signals of synthetic quartz and quartz extracted from ceramics and sediments. Bailiff (2000) observed a time-resolved luminescence off-time decay which could be described using a single exponential function with a lifetime of 40 μs ± 0.6 μs for synthetic quartz and of 33 μs ± 0.3 μs for granular quartz extracted from sediment when measured at room temperature. Later studies supported these observations, with lifetimes usually constrained between 30 μs and 40 μs (e.g. Chithambo and Galloway, 2000; Tsukamoto et al., 2010; Ankjærgaard et al., 2010).

Although time-resolved luminescence measurements on the μs-scale for both natural and synthetic quartz indicate that the luminescence signal decays with a single exponential lifetime in the range of 30–40 μs, measurements of optically stimulated phosphorescence over the millisecond to second timescales have uncovered a more complex behaviour (cf. Ankjægaard and Jain, 2010).

3.2. Sensitisation of quartz luminescence

In 1971, Zimmerman proposed a mechanism explaining changes in quartz luminescence sensitivity: she showed that the 110 °C thermoluminescence (TL) peak of quartz can be sensitised when the sample is beta irradiated and annealed to 500 °C. Contrary, the 110 °C TL signal could be reduced due to exposure to short UV (~250 μm) radiation, whereas subsequent heating to 500 °C would restore the TL intensity. Zimmerman (1971) combined her TL experiments with thermally stimulated exo-electron (TSEE) measurements to understand the physical processes governing the induced changes in quartz 110 °C TL sensitivity.

Based on her experimental observations, Zimmerman (1971) concluded that due to the similarity of the TL and TSEE peaks, the charge captured by the recombination centres are likely to be electrons, with the recombination centres being positively charged. Zimmerman (1971) explains the increase in quartz 110 °C TL, due to initial dosing and annealing to 500 °C, as an increase in the number of luminescence centres. Interestingly, whilst irradiating and heating causes sensitisation of the 110 °C TL peak, UV radiation results in desensitisation. Zimmerman (1971) explained this phenomenon as the UV photons exciting electrons from the valence band to the recombination centres, thus causing transfer of holes. Her concept includes different types of hole centres: luminescent (L-centre) and non-luminescent centres (K-centres) (see also Fig. 4B). According to Zimmerman (1971), exposing a pre-dosed quartz sample to UV radiation causes the excitation of an electron from the valence band into an L-centre. The hole left behind in the valence band will now be transferred to a K-centre.

Heating of the pre-dosed and UV-irradiated quartz will then cause thermal excitation of an electron from the valence band into the K-centre. Subsequently, an electron, previously trapped in an L-centre will move to the valence band, resulting in hole movement from the K-centre to an L-centre. The hole is now trapped at an L-centre. Here an electron can recombine with this hole and result in the emission of luminescence of the thus sensitised quartz.

Whilst Zimmerman (1971) explains sensitisation of quartz TL, Bøtter-Jensen et al. (1995) make use of a similar explanation to describe sensitisation of the OSL signal of quartz. The mechanism proposed by Zimmerman in 1971, and a version adapted by Bøtter-Jensen et al. (1995) provides important background information to understand some interpretations of time-resolved phenomena in quartz due to high temperature annealing.

3.3. Thermal quenching of quartz luminescence and its lifetimes

The complexity of luminescence processes in quartz becomes evident when examining OSL lifetimes, particularly in response to variations in annealing temperature (e.g. Chithmabo et al., 2016; Galloway, 2002; Chithambo et al., 2008), or stimulation temperature (e.g. Bailiff, 2000; Chithambo and Galloway, 2001; Chithambo and Ogundare, 2009). A key question that arises is: how does thermal quenching of the luminescence signal influence the lifetimes measured? This section focusses on understanding this relationship, as it is essential for interpreting time-resolved luminescence data. To explain the observed variations in lifetime under different thermal conditions, two physical models have been proposed: The Schön-Klasens model and the Mott-Seitz model. Both models were originally developed to describe thermal quenching, a process that leads to a reduction in luminescence intensity at elevated temperatures. However, while they aim to explain the same phenomenon, they attribute it to fundamentally different underlying mechanisms. The following sections examine these models in detail, exploring their theoretical foundations and their implications for interpreting thermal quenching in quartz OSL.

The Mott-Seitz model (cf. Guerney and Mott, 1939; Seitz, 1939, cf. Fig. 4) is a one-centre-model for thermal quenching and is explained using a configurational coordinate diagram, including the potentials of a ground and an excited state of the defect (e.g. see Bøtter-Jensen et al., 2003 for detailed explanations; Fig. 4A). According to the Mott-Seitz model, charge (i.e. an electron) is excited within a defect to its excited state. From here two relaxation scenarios are possible: Either the electron can undergo a radiative relaxation from the excited state to the ground state, while emitting luminescence, or the electron can absorb phonon energy to overcome the energy barrier between the minimum of the excited state potential and the intersection of the two potentials. Following Guerney and Mott (1939) this energy difference is denoted as W (Fig. 4A). When following this second process according to the Mott-Seitz model, the transition across the barrier results in a non-radiative transition to the ground state, under the emission of phonons only (Dexter et al., 1955). This means that with increasing stimulation temperature more phonon energy is available to the excited electron, increasing the likelihood of phonon energy absorption to overcome the potential barrier between the excited state minimum and the intersection point, resulting in an increase in non-radiative transitions, compared with the radiative transitions at lower stimulation temperatures. Besides a decrease in luminescence intensity, a change in excited state lifetime (and thus in the luminescence decay time observed from time-resolved OSL) with increasing stimulation temperature is also expected (e.g. Bailiff, 2000; Bøtter-Jensen et al., 2003). A more detailed explanation of the quantum mechanical nature of the processes can be found in the discussions around Fig. 4.2 in Chapter 4 of Chithambo (2018).

According to the Schön-Klasen model (Schön, 1942; Klasens, 1946,

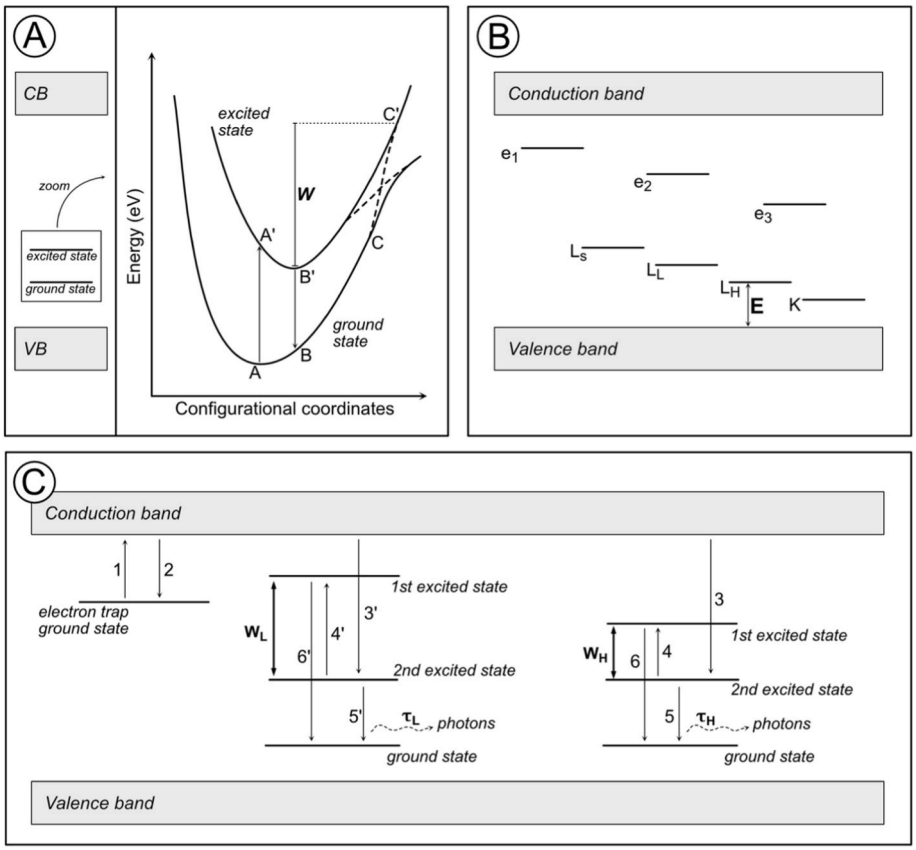

Fig. 4. (A) Mott-Seitz model for thermal quenching within a defect. The intra-defect transitions (between the potentials of the ground and excited state) are shown, as well as the quenching energy W. The figure is based on Guerney and Mott (1939). (B) A band model following Schön-Klasen with three different electron trapping centres and four hole centres. L-centres are luminescence centres, whilst K is a non-luminescence centre. The hole centres are denoted following Galloway (2002). Here the quenching energy E is shown and corresponds to the energy difference between the hole centre and the valence band. E is indicated for L_H. (C) The model proposed by Pagonis et al., (2014). It uses the thermal quenching mechanism following Mott-Seitz, but includes two different recombination centres with different energy levels and lifetimes (τ_L and τ_H) for the resulting luminescence.

cf. Fig. 4B) thermal quenching can be explained by a thermally unstable hole population. At elevated temperatures (referring to temperatures above room temperature, often within the range of a few tens to hundred °C), the trapped holes are released thermally from their trapping centres, resulting in a significant reduction in the number of available recombination sites, leading to quenching of the luminescence signal. Following the described process, whilst observing a reduction in luminescence intensity, no change in lifetime should be observed according to Bøtter-Jensen et al. (2003, p. 45–46).

Whilst originally intended to describe thermal quenching of luminescence during increasing stimulation temperatures, the Schön-Klasens model has widely been used to explain a change in quartz luminescence lifetime observed, when the quartz sample had been exposed to different annealing temperature prior to the time-resolved luminescence measurement (e.g. Galloway, 2002; Chithambo et al., 2011). Further details regarding the application of both models are given below.

The application of both the Mott-Seitz and Schön-Klasens models to describe the decrease in quartz OSL lifetime with increasing stimulation or annealing temperature, combined with the interchangeable use of the variables W and ΔE to represent different energy differences, adds complexity to the interpretation of observed phenomena. In the Mott-Seitz model, W represents the energy required to thermally activate a non-radiative transition, specifically the energy difference between the intersection of the excited and ground state potentials and the minimum of the excited state potential. In contrast, in the Schön-Klasens model, E denotes the energy barrier preventing electron-hole recombination, specifically the energy difference between the ground state of the hole centre and the upper edge of the valence band. To maintain clarity throughout this review, we adopt the convention established by Guerney and Mott (1939), using W to denote the energy difference between the intersection of the potentials and the minimum of the excited state potential in the Mott-Seitz model. In contrast, when discussing the Schön-Klasens framework, we follow the original convention of Klasens (1946) and use E to represent the energy difference between the hole centre and the upper edge of the valence band (Fig. 4B).

Following this, the effect of thermal quenching, on the OSL lifetime (τ), due to an increase in the stimulation temperature, according to the Mott-Seitz model, can be described by (equation (4)):

$$\tau(T_m) = \frac{\tau_0}{1 + C \exp\left(-W/k_B{*}T_m\right)} \quad [4]$$

with τ_0 denoting the lifetime of the radiative transition, C is a constant ($C = s * \tau_0$, with s being the frequency factor), k_B is Boltzmann's constant and T_m the absolute temperature during the measurement.

Following Schön and Klasens, as adapted by Galloway (2002) and by Chithambo et al. (2008) (cf. Fig. 4B), the decrease in lifetime with annealing temperature can generally be described following equation (5):

$$\tau_a = \tau_L + \frac{(\tau_H - \tau_L)}{1 + K \exp\left(-\frac{E}{k_B T_a}\right)} \quad [5]$$

In this equation, τ represents the luminescence lifetime, while T_a denotes the annealing temperature in Kelvin. The parameter K is a constant related to the probability of non-radiative recombination, and E

corresponds to the activation energy above the valence band of a non-radiative recombination centre. The subscripts L and H refer to distinct hole centres (L_L and L_H), each contributing differently to the recombination process. Typically, when luminescence arises from two separate recombination centres, time-resolved OSL measurements exhibit a double-exponential decay, characterised by lifetimes τ_L and τ_H. However, as discussed by Galloway (2002), if the two centres have similar lifetimes, their individual contributions become indistinguishable, and the decay curve cannot be resolved into two separate components. Instead, a single-exponential decay is observed, with an apparent lifetime that represents the weighted average of both contributions. The variation in measured lifetime in such cases does not necessarily reflect a fundamental change in recombination dynamics but rather the limitations of the measurement system in distinguishing closely spaced decay components.

3.4. Dependency of quartz OSL lifetime on stimulation temperature

Bailiff (2000) showed that the lifetime of the time-resolved OSL signal of a synthetic quartz specimen decreases from ~40 μs when measured at ambient temperature to ~10 μs when measured at 220 °C, attributing it to thermal quenching. The observed change in lifetime corresponds to a decrease of ~75 % when measured at elevated temperatures. Similar observations were made by Chithambo and Galloway (2001), who showed that the quartz OSL lifetime remains constant between 293 K and 373 K, followed by a ~75 % decrease in lifetime with measurement temperatures being increased from 373 K to 473 K. Based on the results of multiple studies, it becomes evident that the effect of thermal quenching on the quartz OSL lifetime comes to effect at stimulation temperatures above 373 K (100 °C). Below this temperature, the luminescence lifetimes remain stable at approximately 40 μs. However, at higher temperatures, a decrease in lifetime is observed, which has been attributed to the transition from radiative to non-radiative recombination due to thermal quenching (e.g. Bailiff, 2000; Chithambo and Galloway, 2001; Chithambo and Ogundare, 2009). Fitting the stimulation temperature-dependent time-resolved OSL data for quartz using equation (4) to determine W, yielded values ranging from approximately 0.5 eV–0.8 eV. A compilation of reported values for W (denoted as ΔE in their study) can be found in Table 1 of Chithambo (2003).

3.5. Dependency of quartz OSL lifetime on annealing temperature

Building on earlier reports of increased thermoluminescence (TL) intensity in quartz following high temperature annealing (e.g., Sunta and David, 1982; Watson and Aitken, 1985), Bøtter-Jensen and colleagues (1995) demonstrated that quartz OSL sensitivity is strongly dependent on the annealing temperature. Their study showed that the luminescence response reaches its highest sensitivity after annealing at 800 °C. Similarly, in addition to the enhancement of luminescence sensitivity up to 800 °C, annealing temperature has also been found to influence the luminescence lifetime of quartz. Multiple studies have investigated the relationship between quartz luminescence lifetime and annealing temperature, consistently reporting a decrease in lifetime as annealing temperature increases (e.g. Chithambo, 2002; Galloway, 2002; Chithambo et al., 2008). This decrease in lifetime with increasing annealing temperature is generally well described by equation (5).

Fig. 4B shows a schematic band diagram of quartz with different hole centres denoted S, L and H. According to the interpretation by Galloway (2002) and by Chithambo et al. (2008), annealing of the samples causes transfer of holes from one luminescence centre to another. The interpretation of Galloway (2002) and Chithambo et al. (2008) follows the model proposed by Zimmerman (1971), and its modified version of Bøtter-Jensen et al. (1995) for the change in TL and OSL sensitivity with annealing temperature.

Quartz crystals exhibit phase changes when exposed to prolonged high temperature annealing. These different polymorphs of quartz are stable within different temperature ranges. Interesting for the question regarding the reasons behind the changes in luminescence sensitivity and lifetime of quartz during annealing processes are the phase transitions at 573 °C and 870 °C, where α-Quartz transitions into β-Quartz, and β-Quartz transitions into β-Tridymite, respectively (see Deer et al., 2013, p. 311, for further details).

Bøtter-Jensen et al. (1995) observed an increase in the emission ~380 nm TL and OSL in their emission spectra, with a maximum increase around 800 °C. Others also observed increasing TL and OSL signals in quartz after high temperature irradiation steps: Hashimoto et al. (1994) observed an increase in red and blue TL, but with a more pronounced increase for red TL. Hashimoto et al. (1996) measured a linear increase in blue TL for annealing temperature above 700 °C, together with the creation of a red emission band that grew in strength with annealing temperatures beyond 800 °C. Bøtter-Jensen et al. (1995) recorded emission spectra and revealed that while the blue emission (~450 nm) is relatively unaffected by the sensitisation process, it is primarily the violet emission (~380 nm) which is enhanced. Furthermore they observed a change in TL peak position, both leading the authors to conclude that the experiments caused a change in the hole centre concentrations: According to Bøtter-Jensen et al. (1995), either annealing causes an increase in the number of luminescence centres or a decrease in the number of non-luminescence centres, both resulting in an increase in luminescence.

Similarly, Martini et al. (1995) observed the strong enhancement of the 380 nm quartz TL emission after high-temperature annealing at 1400 °C for 10 h. Martini et al. (1995) suggested that the prolonged heating of the quartz samples caused the reduction of ionic charge compensators (M^+ and H^+, with M^+ referring to cations such as Li^+ and Na^+) at Al sites, which is then compensated by the formation of $[AlO_4]^0$ centres, leading to the TL emission at 380 nm.

From a luminescence physics perspective, changes in luminescence sensitivity and associated lifetime have been attributed to variations in the hole population within different recombination centres. Galloway (2002) proposed that high-temperature annealing induces the transfer of holes from non-luminescent K-centres to the luminescent L_H and L_L levels (Fig. 4B), thereby influencing both sensitivity and lifetime. This explanation is based on the assumption that the different hole centres (L_H and L_L) exhibit distinct luminescence lifetimes. Galloway (2002) interprets this behaviour within the framework of the Schön-Klasens model (equation (5)). Supporting the presence of multiple luminescence centres, Bøtter-Jensen et al. (1995) observed that the thermoluminescence (TL) emission spectrum differs between annealed and unannealed quartz, indicating that annealing affects the nature of the luminescence recombination centres. This further reinforces the hypothesis that high-temperature annealing modifies the population and distribution of charge carriers, thereby altering both luminescence sensitivity and decay kinetics.

3.6. Thermal quenching of quartz OSL lifetimes - A simulation approach

While the just described results are based on experimental observations, Pagonis et al. (2010, 2014) took a different approach and simulated the time-resolved signal of quartz under different conditions. In their 2010 study Pagonis et al. developed a new model describing thermal quenching in quartz time-resolved signals (Fig. 4C). Their model is based on the Mott-Seitz principle for thermal quenching, focusing on the competition between radiative and non-radiative processes within a recombination centre. A later addition to this model included two luminescent recombination centres (L_L and L_H) and the non-luminescent hole centres termed R (Pagonis et al., 2014, cf. Fig. 4C). The updated model enabled the simulation of thermal quenching due to increasing stimulation temperatures, following the Mott-Seitz model, with internal transitions within the L_L and L_H centres. Furthermore, the model allowed for a change in luminescence sensitivity due to thermal

annealing to be examined (see e.g. Chithambo, 2002; Galloway, 2002; Chithambo et al., 2008, for experimental data). For this purpose, the updated version of the model by Pagonis et al. (2014) assumed that annealing of quartz results in the redistribution of holes among L_L and L_H centres. Thus, at ambient temperatures, the concentration of centres with lifetimes of τ_H is believed to be greater than that of centres with lifetimes following τ_L. However, following annealing at temperatures above 500 °C, the number of τ_L centres increases. Consequently, in cases where the decay cannot be resolved into separate components originating from individual luminescence centres, Galloway (2002), the observed lifetime (τ) reflects a single decay constant. At ambient temperature, this lifetime is primarily governed by the slower τ_H, whereas for annealed samples, the faster τ_L becomes the dominant contribution.

Simulation results shown by Pagonis et al. (2014) support experimental observation of both, the effect of increasing stimulation temperature (cf. Chithambo, 2002; Galloway, 2002) and annealing temperature (e.g. Galloway, 2002) on lifetimes of quartz OSL signals obtained using time-resolved measurements.

Chithambo et al. (2016) further review and discuss strengths of combining experimental data and simulation results, not only for understanding thermal quenching in quartz, but also for calculating kinetic parameters of quartz (time-resolved) OSL. We refer the reader to the original review publication for further details.

3.7. Time-resolved optically stimulated phosphorescence of quartz

Whilst the so far in this section explained phenomena and processes have been obtained for time-resolved OSL measurements of quartz on the microsecond timescale, a more complex decay behaviour can be found when time-resolved luminescence measurements are made on longer time scales. Jain and Ankjægaard (2010) performed time-resolved measurements on the millisecond to second timescale, thus constraining lifetimes of the time-resolved optically stimulated phosphorescence (OSP) signal. Based on their experiments Ankjærgaard and Jain (2010a,b) observed time-resolved OSL and OSP decay over eight decades, ranging from 50 ns to 8 s. In their combined signal (Fig. 5) Ankjærgaard and Jain (2010a,b) visually identified four different components governing the quartz luminescence decay. Their fastest lifetime component (component 1 in Fig. 5A and B) is identical to the sole component observed when studying quartz time-resolved OSL on the microsecond time scale (e.g. Bailiff, 2000; Chithambo and Galloway, 2000; Tsukamoto et al., 2010; Ankjærgaard et al., 2010), and can likely be associated with the excited state to ground state transition within the recombination centres. The further components identified exhibit average lifetimes ranging from ~1 ms (component 2, Fig. 5A,B,C) to ~5 s (component 4, Fig. 5A–D). These components have been found to show different behaviour when the luminescence is measured at different temperatures. Component 3 (Fig. 5A–D) exhibits a strong measurement temperature dependence and has shown to originate from photo-transferred TL through the 110 °C trap, in agreement with Wintle and Murray (1997), as well as from other low temperature TL peaks between 87 °C and 165 °C Ankjærgaard and Jain (2010a,b).

3.8. Summary - time-resolved luminescence of quartz

Time-resolved luminescence measurements of quartz provide critical insights into the charge transfer mechanisms and recombination kinetics governing its luminescence behaviour. By analysing the key transitions involved — electron eviction, charge transfer through the conduction band, and relaxation at the recombination centre — this review highlights the factors influencing luminescence lifetimes. Early research established that quartz OSL typically follows a first-order kinetic model, with lifetimes ranging between 30 and 40 μs at room temperature. However, deviations from this simplified model have been observed, particularly because of thermal quenching, thermal annealing, and the presence of multiple recombination centres. These complexities indicate that the traditional one-trap one-luminescence-centre models do not fully account for all the luminescence phenomena exhibited by quartz, necessitating more sophisticated theoretical frameworks.

The effect of thermal quenching on quartz luminescence has been extensively studied, with two primary models, the Mott-Seitz and Schön-Klasens models, proposed to explain the observed reduction in

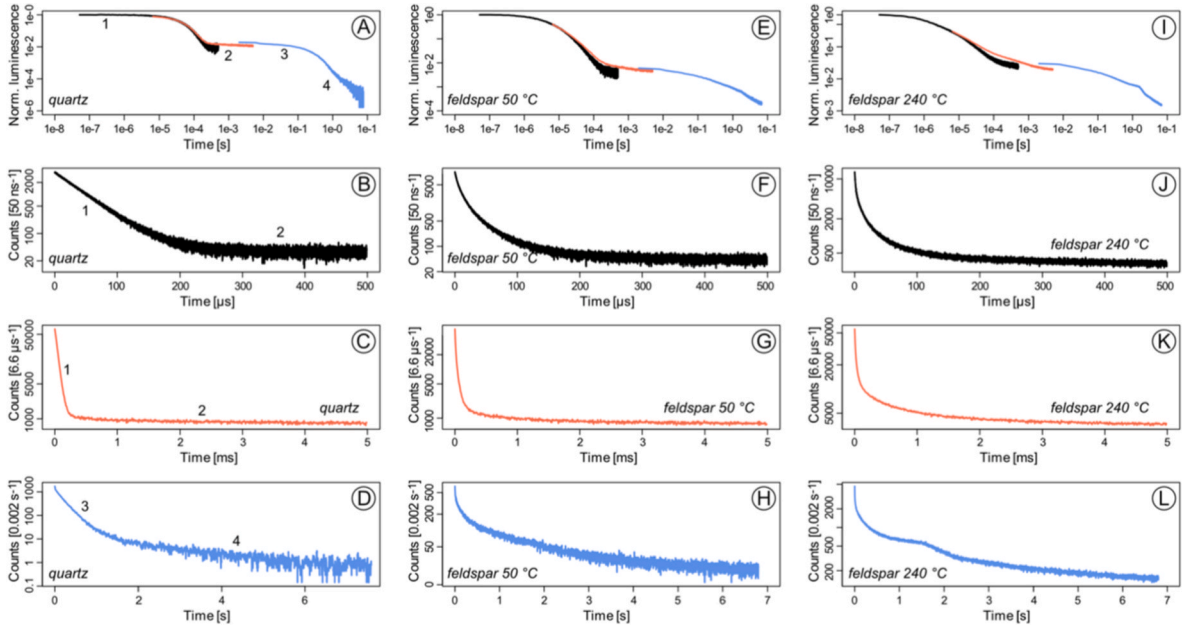

Fig. 5. Time-resolved optically stimulated luminescence (OSL) and optically stimulated phosphorescence (OSP) curves of quartz (A–D) and feldspar (E–L). The figures are adapted from Ankjærgaard and Jain (2010a,b). Figures A, E and I are compilation figures for each signal investigated. For quartz the time-resolved OSL and OSP curves (blue stimulation) are shown in B-D for the different time scales. These curves were obtained after a 10 s preheat at 260 °C. For feldspar time-resolved infrared stimulated luminescence (IRSL) and phosphorescence (IRSP) signals were measured at 50 °C (E–H) and as a post-IR IRSL/IRSP at 240 °C (I–L). Here the preheat temperature was set at 300 °C for 60s. (For interpretation of the references to colour in this figure legend, the reader is referred to the Web version of this article.)

luminescence intensity and lifetime at elevated temperatures. The Mott-Seitz model attributes quenching to a transition from radiative to non-radiative recombination due to increased phonon absorption, while the Schön-Klasens model links quenching to a reduction in available hole centres. Experimental studies, including those by Bailiff (2000), Chithambo and Galloway (2001), and Ankjærgaard and Jain (2010a,b), have shown that quartz luminescence lifetimes remain stable up to ~100 °C, beyond which they decrease significantly due to quenching effects. These findings underscore the importance of considering thermal history in luminescence dating, as failure to account for temperature-dependent lifetime variations may introduce biases in age estimations.

Beyond quenching effects, annealing temperature has also been found to play a crucial role in influencing luminescence sensitivity and lifetime. High-temperature annealing redistributes charge carriers between luminescent and non-luminescent centres, altering both sensitivity and decay kinetics. Notably, annealing quartz at ~800 °C has been linked to enhanced OSL sensitivity, a phenomenon attributed to the transfer of holes from non-luminescent K-centres to luminescent L-centres. This has significant implications for luminescence dating applications involving heated sediments, pottery, and burnt lithics, as it highlights how thermal treatment affects quartz luminescence properties. Moreover, time-resolved measurements on longer timescales (milliseconds to seconds) have revealed multiple decay components, further demonstrating the limitations of simplified kinetic models and emphasizing the need for careful signal separation techniques.

Looking ahead, advancements in time-resolved luminescence methodologies have the potential to enhance the precision of luminescence dating and broaden its applications beyond traditional chronology into fields such as thermochronology (e.g. Herman et al., 2010; Guralnik et al., 2015; Tang and Li, 2015), provenance analysis (e.g. Sawakuchi et al., 2018; Tanski et al., 2024), and sediment transport reconstructions (e.g. Rink, 1999; Gray et al., 2019). So far, it has not been tested, whether the time-resolved signal of quartz could provide further information on rock cooling conditions, provenance settings, or post-crystallisation processes. By integrating experimental data with simulation models, such as those proposed by Pagonis et al. (2014), future research can refine our understanding of charge transfer dynamics and improve the accuracy of luminescence-based dating techniques. Further research could potentially explore whether extending the luminescence model by Bailey (2001, 2004) to also account for processes visible using time-resolved measurements could enhance our understanding of luminescence processes in quartz. Ultimately, a more comprehensive exploration of time-resolved luminescence in quartz—beyond the constraints of simple one-trap one-centre models—will enable a more robust reconstruction of past geological and archaeological events.

4. Time-resolved luminescence of feldspars [$KAlSi_3O_8$ - $NaAlSi_3O_8$ – $CaAl_2Si_2O_8$]

Time-resolved luminescence studies have demonstrated that feldspar luminescence processes are significantly more complex than those observed in quartz. While quartz OSL is often approximated using a OTOR model, time-resolved OSL measurements reveal that this simple framework does not fully capture the observed luminescence behaviour, as discussed in the previous section. In feldspars, the complexity is even more pronounced, as the OTOR model is insufficient to explain time-resolved luminescence phenomena (e.g. Huntley, 2006; Jain et al., 2015; 2015).

On the ns-timescale, some feldspar samples exhibit single-exponential decay components, suggesting that certain recombination pathways operate with well-defined kinetics under specific conditions. However, at longer microsecond timescales, feldspar luminescence decay does not follow a simple exponential function. Instead, it is typically described as a sum of multiple exponentials (e.g. Tsukamoto et al., 2006) or a combination of a single decaying exponential and a stretched exponential function (e.g. Pagonis et al., 2012). Whether these empirical fitting functions accurately represent the underlying charge transfer mechanisms remains an open question. The presence of multiple recombination pathways inherently complicates the interpretation of time-resolved luminescence, particularly in infrared stimulated luminescence (IRSL) measurements.

A key debate in feldspar luminescence research concerns whether IRSL arises from a single type of electron trapping centre or a broad distribution of traps. While earlier studies suggested that a distribution of traps contributes to feldspar IRSL, more recent research favours the single-trap-type hypothesis (e.g. Andersen et al., 2012; Kumar et al., 2020). Despite progress in understanding electron trapping mechanisms, the specific types of crystal defects responsible for charge storage remains unidentified. Similarly, the nature of the recombination centres involved in feldspar luminescence is still partially unresolved. However, time-resolved IRSL measurements have provided valuable insights into the defects and processes governing feldspar luminescence (e.g. Prasad et al., 2016; Prasad and Jain, 2018; Riedesel et al., 2023).

This section explores the fundamental principles of time-resolved feldspar luminescence, discussing the role of multiple recombination pathways, the influence of defect structures, and the broader implications of these findings for luminescence dating applications. By examining the temporal evolution of luminescence signals across different timescales, time-resolved studies continue to refine our understanding of charge transfer mechanisms in feldspars and improve the interpretation of luminescence signals in dating and dosimetry.

4.1. Recombination lifetimes in different feldspars

Luminescence emissions, often recorded as TL or radioluminescence (RL) spectra, or even optically stimulated spectra, of feldspars have been observed in a wide spectral range from the UV to the IR (e.g. Bailiff and Poolton, 1991; Huntley et al., 1991; Krbetschek et al., 1997; Riedesel et al., 2021). Most time-resolved studies have focused on trying to link certain emission with potential defects in the crystal (e.g. Clark and Bailiff, 1998; Prasad et al., 2016; Prasad and Jain, 2018; Riedesel et al., 2023). However, this has been challenged by the different timescales covered and the different emissions observed, which are often broad and featureless (cf. Riedesel et al., 2021).

The first to perform time-resolved luminescence measurements of feldspars were Sanderson and Clark (1994). They were able to measure the blue light (470 nm) stimulated pulsed luminescence (UV emission) of their feldspar samples with a resolution of ~20 ns. Based on their experimental results, Sanderson and Clark (1994) showed that recombination in feldspars takes place on time scales between 100 ns and 10 μs. It should be noted that the line spectrum and the individual peaks observed by Sanderson and Clark (1994) are an artefact of the experimental set-up, such as saturation effects. Clark et al. (1997) observed a similar multi-peak structure in their initial experiments (see their Fig. 3) and associated the two peaks recorded in their measurement as an artefact of the signal processing system.

Clark et al. (1997) presented time-resolved data for a larger suite of samples, comprised of a range of single crystal feldspar specimens. Already in this study, feldspar luminescence lifetimes for three different emission windows (280–380 nm, 350–575 nm, 460–625 nm) were obtained, showcasing the multiplicity of feldspar luminescence decay. Clark et al. (1997) obtained lifetimes ranging from 30 ns to >15 μs, which they were able to group into five defined groups: 30–50 ns, 300–500 ns, 1–2 μs ~5 μs and >10 μs. Interestingly, lifetimes of each group were found in all emission detection bands, but the number of lifetimes obtained for the respective band was found to be sample dependent. This was later supported by Ankjærgaard et al. (2009). Furthermore Clark et al. (1997) found little to no correlation between the lifetimes measured and the chemical composition of the samples.

Due to broad emission bands observed for feldspars (e.g. Bailiff and

Poolton, 1991; Huntley et al., 1991; Krbetschek et al., 1997; Riedesel et al., 2021), Clark et al. (1997) suggested that the multiplicity of the off-time decay observed could be attributed to overlapping emissions. To further investigate this, Clark and Bailiff (1998) recorded their time-resolved luminescence through narrow interference filters. By comparing lifetimes (ranging from a few tens of ns to tens of μs) obtained from time-resolved luminescence measurements with infrared stimulated emission spectroscopy, Clark and Bailiff (1998) conclude that the probed luminescence centres seem to be governed by lattice hole defects resulting in the formation of bridges, such as Al-O-Al bridges, and that luminescence resulting from metal ions, such as Mn^{2+} play a minor role.

The recombination lifetime of the blue (~410 nm) emission in the off-time decay (e.g. Clark and Bailiff, 1998; Riedesel et al., 2023) and its association to a lattice site defect is supported by results from electron paramagnetic resonance (Speit and Lehmann, 1982; Finch and Klein, 1999), by polarisation experiments in excitation-emission spectroscopy (Short, 2004), and by disordering experiments indicating a strong effect of lattice disorder on the intensity, TL curve shape, fading and the lifetime of the blue emission of feldspars (Riedesel et al., 2021, 2023). In these lattice disordering experiments, natural feldspar samples were exposed to prolonged heating at 1050 °C, which disordered the lattice site occupation of Al^{3+} and Si^{4+} ions. Rapid cooling to room temperature of the heated material retains the disordered structure and results in the artificial creation of sanidine feldspars. Interestingly, this artificial disordering results in a significant increase in luminescence lifetimes of the blue TL emission and changes the blue time-resolved IRSL from a multi-exponential decay to a single exponential decay. Whilst ordered specimen exhibit lifetimes in four groups: <1 μs, 3–9 μs, 12–16 μs and lifetimes >20 μs, only lifetimes ~45 μs were observed for the disordered specimen, indicating either a change into the recombination centre emitting blue luminescence or to the charge recombination process (Riedesel et al., 2023).

Whilst the blue emission occurs with lifetimes on the μs-scale, longer lifetimes, on the ms-scale, have been observed for the yellow-green and the red emission (Prasad et al., 2016; Prasad and Jain, 2018). Long lifetimes observed for luminescence phenomena have been related to transition metals, such as Mn or Fe. In transition metal ions, such as Fe^{3+} or Mn^{2+}, the 3d orbitals are of importance when studying luminescence phenomena.

Electronic transitions involving d-orbitals are complex and various reasons can account for the long lifetimes: (1) Transitions of electrons can be spin-forbidden, requiring that electrons reverse their spin for the transition to be permitted (e.g. an up-spin electron would need to turn to a down-spin electron, e.g. Miessler et al.). Since the transition probability is low, the lifetime is increased (e.g. Housecroft and Sharpe, 2018). (2) d-d transitions are parity-forbidden. Parity describes a symmetry property of a system in relation to a centre of inversion. According to the Laporte selection rule, which applies to centrosymmetric systems, no electronic transitions can occur, if no change in parity occurs. Meaning allowed transitions involve g ↔ u (g for the German word *gerade* and u for *ungerade*), but g ↔ g} and u ↔ u are forbidden (Miessler et al.).

(3) Spin selection rule: $\Delta S = 0$. The low probability of an intersystem crossing for the electronic transition, that is a transition involving two electronic states of different spin multiplicity, can lead to long lifetimes. This is for example the case if the electron transitions from a singlet excited state to a triplet ground state. Here the spin of the transitioning electron needs to be reversed for this transition to occur, which makes it a spin-forbidden transition (e.g. Harris and Bertolucci, 1989; Housecroft and Sharpe, 2018). However, it should be noted that electron transitions involving intersystem crossings are radiationless (e.g. Housecroft and Sharpe, 2018).

There are further complexities potentially influencing electronic transitions and lifetimes, such as ligand field effects. We will not go into further detail here, but would like to note that different theories exist, aiming at explaining these complexities, for example crystal field theory, molecular orbital theory and ligand field theory. We would like to refer the reader to textbooks and review papers which outline these details and from which the above explanations have been retrieved: for example, Miessler et al., Housecroft and Sharpe (2018), Schlag et al. (1971), and Harris and Bertolucci (1989).

4.2. Processes governing luminescence lifetimes in feldspars

The complexity of time-resolved luminescence of feldspars and the variety of lifetimes observed for different emissions in feldspars draw us to the question of understanding the different processes governing luminescence phenomena and their lifetimes. Earlier in this review we outlined that essentially three processes influence the lifetime: (1) detrapping of trapped electrons from the electron trap, (2) transition of the detrapped electron to the recombination centre, and (3) relaxation of the electron from the excited state of the recombination centre to its ground state (excited state lifetime). The different scales on which lifetimes are observed for feldspars raise the question, which of these processes is the dominant one.

Using time-resolved luminescence and phosphorescence measurements Ankjærgaard and Jain (2010a,b) and Jain et al. (2015) investigate the processes governing charge eviction, transition and relaxation. Fig. 5F shows the time-resolved luminescence signals of an orthoclase feldspar measured on the μs-scale. In comparison to quartz (cf. Fig. 3 and 5C) the time-resolved luminescence signal of feldspar decays faster. However, similarly to quartz, feldspar also exhibits a time-resolved luminescence signal on the ms-scale, as well as a very slowly decaying phosphorescence signal on the second timescale (cf. Fig. 5G, H, K, J). By investigating the temperature dependency of the slow time-resolved luminescence signal (ms-scale), Ankjærgaard and Jain (2010a,b) infer that this slowly decaying signal originates from emptying of the sub-conduction band-tail states, followed by electron-hole recombination (Fig. 6). This intensity of the signal on the ms-scale from the band-tail states has a lower intensity than the signal on the μs-scale.

Based on their time-resolved data, obtained by stimulating with different photon energies, and different thermal (pre-)treatments, Jain et al. (2015) developed a comprehensive model for feldspars, which shows that the lifetimes measured for feldspar IR, green, and blue stimulated luminescence are primarily governed by the process of

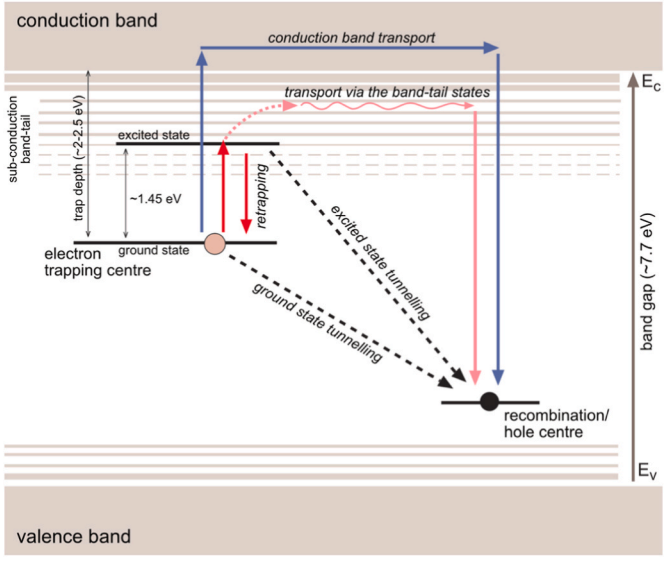

Fig. 6. Energy band diagram of feldspar, drawn schematically with one electron and one hole trapping centre. The figure also shows different electron-hole recombination pathways, either via the conduction band, the sub-conduction band-tail states or as direct transitions from either the ground or the excited state of the electron trapping centre to the recombination centre. The recombination centre is displayed with a single energy level for simplicity reasons.

recombination and that the route taken by the electrons to recombine with a hole centre dictate the lifetime. The routes taken have been shown to be dependent on the excitation energy of the optical stimulation. Key to their interpretation is the observation of a 'fast' and a 'slow' signal, with these signals not only governing different time scales, but also being affected by thermal (pre-) treatments to a different degree. Whilst they relate the fast signal to tunnelling of electrons from the excited state of the electron trap to the recombination centre, the so-called 'slow' signal is thought to result from recombination via the band-tail states. With the knowledge gained from their extensive time-resolved experiments, Jain et al. (2015) made suggestions regarding the optimal isolation of a feldspar luminescence signal that exhibits less fading for more useful for dating applications.

Jain et al. (2015) and Jain et al. (2015) developed a mathematical model for feldspar luminescence, which is based on a random distribution of defects. The model describes feldspar luminescence as the product of localised electron-hole recombination via excited state tunnelling within randomly distributed donor-acceptor pairs, with the tunnelling distance dependent on the defect density. Pagonis et al. (2016) tested the applicability of this localised transition model to time-resolved luminescence data on the μs timescale. They find that the fit of the model to experimental time-resolved data depends on the degree of retrapping, the amount of charge still trapped in defects, and thus on the length of the excitation pulse as well as on the part of the POSL curve examined (early in the experiment vs late in the experiment). Additionally, the authors interpret deviations of the experimental data from the predicted data using the findings of Jain et al. (2015), according to which transition via the band-tail states is another possible recombination route, which however, cannot be described by the model of Jain et al. (2015) and Jain et al. (2015). Further modelling-based approaches to better understand luminescence production in feldspars have been conducted. Pagonis and Kulp (2017) translated analytical equations, based on the feldspar fading model by Larsen et al. (2009), into a Monte Carlo approach, which showed promising results when compared to experimental data, including feldspar time-resolved luminescence data. Further Monte Carlo based approaches which describe feldspar luminescence signals exist (e.g. Pagonis et al., 2017a,b), but have not focussed on time-resolved luminescence signals yet. These Monte Carlo-based approaches have been used to perform simulations of three types of recombination systems: (i) delocalised transitions (e.g. Mandowski and Świątek, 1998), (ii) localised transitions (e.g. Pagonis et al., 2019), and (iii) models, which include both localised and delocalised transitions (e.g. Mandowski, 2004; Mandowski, 2008). Despite the different recombination routes considered by these models, they all simulate electron-hole recombination. In contrast, Spooner et al. (2024) and Williams and Spooner (2025) propose an alternative mechanism to explain time-resolved luminescence behaviour. Similarly to Jain et al. (2015), Spooner et al. (2024) and Williams and Spooner (2025) observe fast and slow decaying time-resolved luminescence signals. However, they propose an alternative explanation for their observed fast and slow decaying time-resolved signals, which is based on a defect-pair model (cf. Itoh et al., 2001, 2002). According to this model, luminescence can be explained by the exchange of different types of impurities or defects, such as electrons, holes, and ions, rather than electron-hole recombination only. Whilst Spooner et al. (2024) and Williams and Spooner (2025) concur with Jain et al. (2015) on the fast time-resolved signal to originate from electron-hole recombination, the slow signal is interpreted as resulting from the movement of an alkali ion, which is argued to be less mobile and consequently slower than an electronic transition. The contribution of each component (electron and ion) varies between the different samples examined (Spooner et al., 2024; Williams and Spooner, 2025). This alternative view on luminescence production in feldspars presented by Spooner et al. (2024) and Williams and Spooner (2025) could spark new simulation initiatives into further exploring luminescence productions in feldspars.

4.3. Dependence of time-resolved luminescence on feldspar chemistry and structure

Feldspars constitute a chemically and structurally diverse mineral group, with variations that can significantly influence their luminescence properties. Consequently, it is essential to characterise the specific feldspar samples under investigation before conducting time-resolved luminescence experiments. Such characterization ensures a more accurate interpretation of the physical processes governing luminescence phenomena, including emission spectra, luminescence intensities, and lifetimes.

Infrared stimulated photoluminescence (IRPL, Prasad et al., 2017) allows the direct probing of electrons trapped within electron trapping centres, thought to be involved in feldspar IRSL. The IRPL signal arises due to retrapping of optically excited electrons within the electron trapping centre (see Fig. 6). Measuring the time-resolved IRPL signal will thus give information on the excited state lifetimes of these electron traps.

Prasad et al. (2017) were the first to report lifetimes for the excited state of these electron trapping centres, constraining them to ~30 μs and ~40 μs, depending on the measurement temperature (295 K versus to 7 K). Later, Kumar et al. (2020) constrained the lifetime of the IRPL signal, resulting in similar lifetimes of ~20 μs–~25 μs. Riedesel et al. (2023) constrained lifetimes for the time-resolved IRPL signal for eleven chemically and structurally different feldspars at room temperature and observed striking similarities between the measurements of the different samples. For the two IRPL signals measured (referred to as $IRPL_{880}$ and $IRPL_{955}$), two lifetimes ranging from 2 μs to 6 μs and from 7 μs to 22 μs, for $IRPL_{880}$, and from 2 μs to 7 μs and from 8 μs to 25 μs, for $IRPL_{955}$ were observed. For the longer lifetime, which shows an average lifetime of ~20 μs, a weak decreasing trend in lifetimes with increasing K-feldspar component of the respective samples can be observed.

Time-resolved IRSL measurements have consistently revealed luminescence lifetimes on the μs -timescale, with values ranging from <1 μs to >20 μs. Jain et al. (2015) interpreted these lifetimes as representing the time required for electrons to either tunnel directly from the excited state of the electron trap to the recombination centre or to follow a longer, indirect pathway through band-tail states before recombination occurs (see transitions in Fig. 6). The key premise supporting this interpretation is that the measured lifetimes in feldspar time-resolved IRSL and OSL (green and blue stimulated) primarily reflect the time taken for electrons to transition through these pathways, rather than the intrinsic excited-state lifetime of the recombination centre itself. This conclusion is based on experimental observations that show a strong dependence of the recombination dynamics on the excitation photon energy, as well as the presence of multiple competing charge transport mechanisms (Jain et al., 2015). Specifically, for non-resonant excitations, electrons are first promoted to the conduction band, from where they either recombine quickly or become trapped in band-tail states. Once trapped, their recombination follows two competing thermally dependent pathways: a rapid phonon-assisted transition or a much slower tunnelling process from deep band-tail states. Because these transport mechanisms dictate how quickly charge carriers reach the recombination centre, they ultimately control the observed luminescence lifetimes, rather than the lifetime of an excited electron within the recombination centre itself. This interpretation contrasts sharply with the case of quartz, where the recombination centre plays a dominant role in defining luminescence lifetimes. In quartz, the lifetime of the excited state within the recombination centre is the primary factor governing decay kinetics.

Whilst most feldspar samples studied so far exhibit lifetimes of the blue emission ranging from <1 μs to >20 μs, Riedesel et al. (2023) were able to show that changes to the structural state of the feldspar can have a significant impact on the lifetime of the measured blue emission (cf. Fig. 7). Disordering Si- and Al-tetrahedra on the framework of different feldspars results in an increase in lifetime for the on- and off-time signal

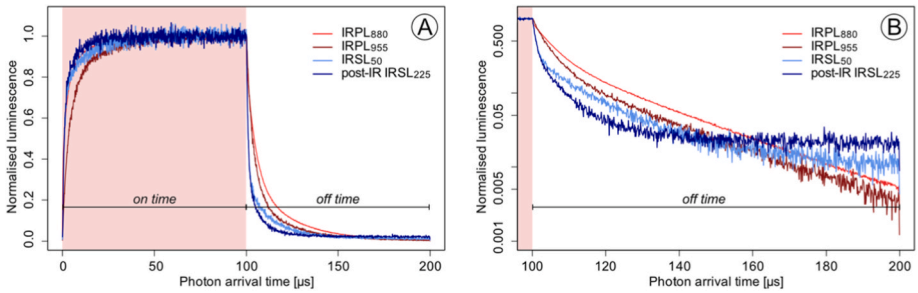

Fig. 7. (A) Summed photon arrival time distributions of the $IRPL_{880}$, $IRPL_{955}$, $IRSL_{50}$, and post-IR $IRSL_{225}$ of a single crystal alkali feldspar. The time-resolved IRPL signals shown here we stimulated using an IR (830 nm) 140 mW TTL modulated laser. (B) The time-resolved signals from A measured during the off-time period, with the intensity on a logarithmic scale.

of about one magnitude. These disordered samples exhibit lifetimes of the blue time-resolved IRSL emission of ~40 μs. It is unclear, if this slowing of the signal results from an enhanced band-tail state transition over excited state tunnelling, or if the changes to the lattice have impacted the recombination centre and its excited state lifetime directly (Riedesel et al., 2023).

Nevertheless, by comparing excited state lifetimes constrained for the electron trapping centres in feldspars to lifetimes measured for the IRSL signal (Fig. 7) different crucial observations can be made: (i) The fast transitions seen in the time-resolved IRSL signal (Clark et al., 1997; Tsukamoto et al., 2006) occur over shorter time-scales than the excited state lifetime of the electron trapping centres, determined by time-resolved IRPL, (ii) the slower transitions as measured in the time-resolved IRSL signal (Ankjærgaard and Jain, 2010a,b; Riedesel et al., 2023) are slower than the excited state lifetime of the electron trapping centre. The longer excited state lifetimes of the electron trapping centres enable recombination via excited state tunnelling, as well as via the band-tail states (Riedesel et al., 2023). However, the long lifetimes (i.e. ~40 μs of the disordered samples in Riedesel et al., 2023, and the lifetimes on the ms-scale observed by Ankjærgaard and Jain, 2010a, b) require further investigations.

4.4. Summary

Time-resolved luminescence is a powerful tool for investigating feldspar luminescence processes, providing insights into variations in emission lifetimes, electron-hole recombination mechanisms, and the influence of feldspar chemistry and structure. These studies have demonstrated that feldspar luminescence cannot be explained by a simple one-trap–one-recombination-centre model, as multiple recombination pathways operate across different timescales. Lifetimes range from nanoseconds to milliseconds, depending on the recombination route. While the blue emission is linked to lattice defects exhibit lifetimes between <1 μs and >20 μs, longer yellow-green and red emissions occur on the millisecond timescale and are associated with transition metals such as Fe or Mn.

A key finding is that the microsecond-scale lifetimes in feldspar time-resolved IRSL and OSL (green and blue stimulated) is thought to primarily reflect electron transport through band-tail states, rather than the excited-state lifetime of the recombination centre. The dependence of recombination on excitation photon energy and pre-treatment conditions supports this interpretation, as different excitation energies favour direct recombination, excited-state tunnelling, or band-tail state transport. These findings are critical for luminescence dating, as they offer new ways to reduce anomalous fading and isolate more stable feldspar luminescence signals.

Despite these advances, open questions remain. The role of excited-state lifetimes in feldspar IRSL, particularly for long-lived signals in disordered feldspars (Riedesel et al., 2021), requires further investigation. Additionally, the impact of lattice disorder on luminescence lifetimes highlights the need for further research into the relationship between feldspar structure, charge transport, and luminescence stability. Similarly to quartz, variations observed in the lifetimes of chemically and structurally different feldspars, may potentially open new research alleys, particularly in the field of luminescence provenance studies (e.g. Scholonek and Augustsson, 2016; Sawakuchi et al., 2018; del Río et al., 2021). Time-resolved luminescence measurements could provide information on cooling temperatures and conditions, due to their sensitivity to the degree of order on the Si,Al-framework (Riedesel et al., 2021), which might prove useful for feldspar luminescence thermochronometry (e.g. King et al., 2016) or palaeothermometry (e.g. Biswas et al., 2020). Furthermore, linking experimental time-resolved luminescence measurements of different emissions with theoretical considerations and models (e.g. Jain et al., 2015; Jain et al., 2015; Spooner et al., 2024) may help to enhance the reliability of feldspar luminescence dating and improve our understanding of charge transfer mechanisms in complex mineral systems.

5. Pulsed stimulation and its application in luminescence dating studies

The luminescence signal obtained from pulsed stimulation, even without time-tagging the photons, has advantages over the routinely used continuous wave stimulated luminescence signal.

In particular, there are two applications in which the pulsed luminescence signal is advantageous: (1) In the case where quartz is the sought mineral for dating, but the sample is unfortunately contaminated by the presence of feldspar. (2) In the case where feldspar is the only option (i.e. when insufficient quartz material is available or when the quartz luminescence signal is of insufficient quality for dating. For this situation a feldspar luminescence signal is required, which can be reset by sunlight, but which also shows minimal fading. The following two examples of application illustrate how pulsed stimulation can assist dating measurements in these cases.

5.1. Pulsed stimulation to discriminate between luminescence emitted by quartz and feldspar

To understand how the application of pulsed OSL can help to discriminate between OSL signals arising from quartz and feldspar grains in a mixed sample aimed for luminescence dating applications, the fundamental differences between the quartz and feldspar luminescence signals obtained under CW and pulsed stimulation need to be explained. When stimulated using blue-LED based CW light the quartz OSL signal, particularly the so-called fast component, decays to a stable background level within the first few seconds after exposure to blue LED light (cf. Fig. 8B). In contrast, the feldspar OSL and IRSL signal needs tens of seconds to decay to the same background level (cf. Fig. 3B and E, Fig. 8B). Neatly, when comparing the time-resolved luminescence signals, particularly the photon-arrival time distributions (cf. Fig. 3C and

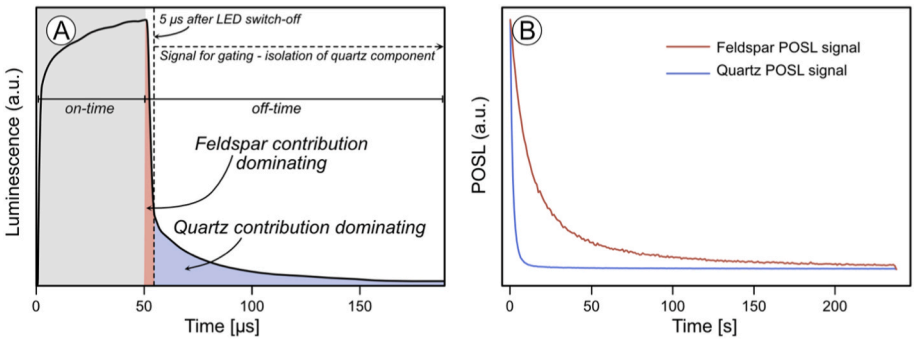

Fig. 8. (A) Time-resolved luminescence signal (re-drawn from Denby et al., 2006) of a quartz and feldspar mixture. From the signal it is evident that feldspar dominates the fast-decaying part of the off-time signal, whilst quartz shows the slower decay. (B) POSL curves of quartz and feldspar sediment extracts. By excluding the initial 5 µs of the off-time, Ankjærgaard et al. (2010) showed that the much faster quartz POSL signal can be isolated. The POSL curves of quartz and feldspar sediment extracts shown here, are displayed for orientation purposes.

F), quartz and feldspar, again, show very different behaviour. The blue stimulated luminescence signal of quartz, recorded in the UV, exhibits lifetimes of ~40 µs, whilst lifetimes for feldspar decay within a few µs, with some parts of the signal even decaying within the first µs or ns (cf. Clark et al., 1997; Clark and Bailiff, 1998). These characteristics enable us to isolate the luminescence signal originating from quartz, by using pulsed stimulation. This has first been proposed by Bailiff and Mikhailik (2003) and was further investigated by Denby et al. (2006), Thomsen et al. (2008), and Ankjærgaard et al. (2010). Since the feldspar luminescence signal decays much faster than the quartz signal, its influence on the quartz luminescence signal can be minimised by excluding the first µs from the off-time signal. Practically this can be done by gating the desired signal in pulsed luminescence. Gating the signal allows for selecting the desired parts of the off-time to be recorded as signal, which can then be treated like a luminescence decay curve (similarly to CW-luminescence, just recorded in the off-time), from which initial parts can be selected as signal, and later parts as background.

Dependent on the sample, an appropriate gating interval should be chosen. Fig. 8A provides an example of how photon-arrival time distributions of a quartz and feldspar mixture would look like. The red-shaded area indicates the off-time signal of the mixture that is dominated by the feldspar signal. The blue area reveals the quartz signal, showing its much slower decay. Fig. 8B shows the obtained POSL signal of respective quartz and feldspar luminescence signals. The stimulated signal (as also known from CW-stimulation) of quartz decays much faster than the signal emitted by the feldspar sample. Combining this information and the shaded areas highlighted in the photon arrival time distribution of the mixed sample in Fig. 8A can help in isolating the quartz-dominated part of the signal and how described gating intervals, as well as signal and background integration can be used in pulsed OSL studies to minimise the impact of feldspar luminescence on the desired quartz luminescence signal. Based on the behaviours studied for different quartz and feldspar samples, Ankjærgaard et al. (2010) suggested discarding the initial 5 µs of the off-time signal (cf. Fig. 8A), to remove substantial proportion of the feldspar luminescence signal. Furthermore, to enhance the quartz luminescence signal contribution, Ankjærgaard et al. (2010) proposed a short on-time period of 50 µs to avoid significant bleaching of the 'fast' OSL decay signal during the on-time stimulation period. From the gated off-time signals, it is suggested that the signal measured during the initial 0.4 µs is integrated, and the later portion of signal used as the background.

5.2. Isolation of a more stable feldspar infrared stimulated luminescence signal

In luminescence dating applications it is important that the luminescence signal used is stable over the timescale of interest, thus over multiple tens to hundreds of thousands of years. Quartz OSL signals originate from so-called deep traps, which have a high thermal and athermal stability, meaning that the electron trapped in these deep electron traps will reside there over geological timescales. The eviction of these trapped electrons requires optical stimulation using higher energies, due to a trap depth of ~3 eV (e.g. Huntley et al., 1996).

Although it has been shown that the electron traps relevant for feldspar IRSL dating have ground state energies of 2–2.5 eV (Hütt et al., 1988; Kars et al., 2013; Riedesel et al., 2019, see Fig. 6), the electrons trapped in these electron traps are not always stable over geological timescales. Most feldspar samples exhibit a loss of charge over time, likely due to quantum mechanical tunnelling of electrons from the ground state of the electron trap to a nearby recombination centre. This unwanted loss of charge is termed anomalous fading. Fading can lead to age underestimation and thus impact the luminescence age calculated significantly. Much effort has been put into either developing reliable fading correction methods (e.g. Huntley and Lamothe, 2001; Huntley, 2006; Kars et al., 2008) or by circumventing fading through adapting measurement protocols to isolate a more stable signal (Thomsen et al., 2008; Li and Li, 2011; Buylaert et al., 2012; Tsukamoto et al., 2017). The most routinely used measurement protocol, which minimises fading, is the post-infrared infrared stimulated luminescence protocol. It measures two consecutive feldspar IRSL signals, with the second one being recorded at temperatures higher than the first IRSL signal. The second signal is referred to as post-IR IRSL signal and is understood to arise from more distant electron-hole pairs, thus isolating a signal less affected by fading (e.g. Jain et al., 2015).

Another method proposed to isolate a more stable signal for dating employs pulsed stimulation. Studying the stability of the different lifetime components for the feldspar time-resolved IRSL signal during the off-time measured a) immediately following irradiation and b) after storing the irradiated samples for 30 days, revealed that different parts of the off-time signal exhibited different rates of fading. With the longest lifetime component in feldspar IRSL (~20 µs) showing greater stability compared to the faster decaying components (Tsukamoto et al., 2006). Due to its better optical bleachability, pulsed IRSL can be favoured over the often used higher temperature post-IR IRSL signals (e.g. Tsukamoto et al., 2017), and some studies have successfully applied the pulsed IRSL signal measured at a sample temperature of 50 °C to date Holocene and Pleistocene sediments (e.g. Roskosch et al., 2015a, b; Tsukamoto et al., 2017), and it has even been shown that a pulsed post-IR IRSL signal can be used as an alternative dating technique (Zhang et al., 2023).

However, these studies have also found that the pulsed signal of feldspars still exhibited some degree of fading (e.g. Jain et al., 2015; Zhang et al., 2023). Zhang et al. (2023) observed fading rates of 0.5–1.1 %/decade for polymineral fine grains and 1.2–1.4 %/decade in the case of sand-sized K-rich feldspar samples (Zhang et al., 2023). Despite these low fading rates measured for the pulsed IRSL signal of some samples, the pulsed IRSL or pulsed post-IR IRSL signal has been shown to be a

good alternative to the post-IR IRSL signal when dating sediments from different geomorphological contexts: The pulsed IRSL signal simultaneously extracts a feldspar luminescence signal with a lower fading rate and a satisfactory bleaching rate.

6. Conclusions

This review has given practical guidance for conducting time-resolved luminescence measurements, with a focus on the two principal experimental approaches: multi-channel scaling and time-correlated single photon counting (TCSPC). Using quartz and feldspars as examples, we highlighted the types of information which can be extracted from time-resolved luminescence measurements of natural minerals.

Summarising the key findings of time-resolved and pulsed OSL studies of quartz and feldspars shows that quartz luminescence is influenced by thermal quenching, annealing effects, and the coexistence of multiple recombination centres, leading to deviations from first-order kinetics. Feldspar luminescence reflects a broader range of recombination pathways spanning nanosecond to millisecond timescales. In both minerals, luminescence lifetimes are strongly influenced by their thermal history, structural disorder, and charge transport mechanisms, underscoring the need for advanced theoretical frameworks that integrate experimental observations with simulation-based models.

Pulsed stimulation has also proven valuable in applied contexts. It enhances the discrimination between quartz and feldspar signals, which is useful when physical separation techniques, such as heavy liquid or magnetic separation, are insufficient. Additionally, pulsed IRSL can isolate a more stable feldspar luminescence signal for dating Pleistocene and Holocene deposits, while ensuring that the signal is sufficiently reset by sunlight. These approaches improve the reliability of luminescence dating across a wide range of geomorphological settings, where conventional signals may be affected by fading or incomplete separation or bleaching.

Overall, this review demonstrates that time-resolved measurements and pulsed stimulation, not only improve signal separation but also expand the applicability of luminescence dating to more complex geological contexts. Continued refinement of our understanding of charge transfer and recombination dynamics in quartz and feldspar will ultimately enhance the precision and robustness of luminescence-based chronologies.

CRediT authorship contribution statement

Svenja Riedesel: Writing – review & editing, Writing – original draft, Visualization, Investigation, Funding acquisition, Conceptualization. **Christina Ankjærgaard:** Writing – review & editing, Writing – original draft, Investigation, Conceptualization.

Declaration of competing interest

The authors declare the following financial interests/personal relationships which may be considered as potential competing interests: Svenja Riedesel reports financial support was provided by European Commission. If there are other authors, they declare that they have no known competing financial interests or personal relationships that could have appeared to influence the work reported in this paper.

Acknowledgements

We would like to thank Alicja Chruścińska (Nikolaus-Kopernikus University Toruń) and Ian Bailiff (Durham University) for valuable feedback on an earlier version of this manuscript. We thank Lars Peter Pirtzel (Technical University of Denmark) for performing the oscilloscope measurements. We would like to thank two anonymous reviewers whose comments helped us to improve this manuscript.

SR acknowledges funding by the EU HORIZON EUROPE Marie Skłodowska-Curie Actions programme (grant no. 101103587).

Data availability

No data was used for the research described in the article.

References

Ankjærgaard, C., Jain, M., Kalchgruber, R., Lapp, T., Klein, D., McKeever, S.W.S., Murray, A.S., Morthekai, P., 2009. Further investigations into pulsed optically stimulated luminescence from feldspars using blue and green light. Radiat. Meas. 44, 576–581.

Ankjærgaard, C., Jain, M., 2010a. Optically stimulated phosphorescence in quartz over the millisecond to second time scale: insights into the role of shallow traps in delaying luminescent recombination. J. Phys. Appl. Phys. 43, 255502. https://doi.org/10.1088/0022-3727/43/25/255502.

Ankjærgaard, C., Jain, M., 2010b. Optically stimulated phosphorescence in orthoclase feldspar over the millisecond to second time scale. J. Lumin. 130, 2346–2355. https://doi.org/10.1016/j.jlumin.2010.07.016.

Ankjærgaard, C., Jain, M., Thomsen, K.J., Murray, A.S., 2010. Optimising the separation of quartz and feldspar optically stimulated luminescence using pulsed excitation. Radiat. Meas. 45, 778–785.

Bailey, R.-M., 2001. Towards a general kinetic model for optically and thermally stimulated luminescence of quartz. Radiat. Meas. 33, 17–45.

Bailey, R.M., 2004. Paper I – simulation of dose absorption in quartz over geological timescales and its implications for the precision and accuracy of optical dating. Radiat. Meas. 38, 299–310.

Bailiff, I.K., Poolton, N.R.J., 1991. Studies of charge transfer mechanisms in feldspars. Nucl. Tracks Radiat. Meas. 18, 111–118.

Bailiff, I.K., 2000. Characteristics of time-resolved luminescence in quartz. Radiat. Meas. 32, 401–405.

Bailiff, I.K., Mikhailik, V.B., 2003. Spatially-resolved measurement of optically stimulated luminescence and time-resolved luminescence. Radiat. Meas. 37, 151–159.

Biswas, R.H., Herman, F., King, G.E., Lehmann, B., Singhvi, A.K., 2020. Surface paleothermometry using low-temperature thermoluminescence of feldspar. Climate oft he Past 16, 2075–2093. https://doi.org/10.5194/cp-16-2075-2020.

Bøtter-Jensen, L., Duller, G.A.T., Poolton, N.R.J., 1994. Excitation and emission spectroscopy of stimulated luminescence from quartz and feldspars. Radiat. Meas. 23, 613–616.

Bøtter-Jensen, L., Agersnap Larsen, N., Mejdahl, V., Poolton, N.R.J., Morris, M.F., McKeever, S.W.S., 1995. Luminescence sensitivity changes in quartz as a result of annealing. Radiat. Meas. 24, 535–541.

Bøtter-Jensen, L., McKeever, S.W.S., Wintle, A.G., 2003. Optically Stimulated Luminescence Dosimetry. Elsevier Science B.V., Amsterdam, the Netherlands.

Chen, R., Hornyak, W.F., Mathur, V.K., 1990. Competition between excitation and bleaching of thermoluminescence. J. Phys. Appl. Phys. 23, 724–728.

Chithambo, M.L., Galloway, R.B., 2000. Temperature dependence of luminescence time-resolved spectra from quartz. Radiat. Meas. 32, 627–632.

Chithambo, M.L., Galloway, R.B., 2001. On the slow component of luminescence stimulated from quartz by pulsed blue light-emitting diodes. Nucl. Instrum. Methods Phys. Res. B 183, 358–368.

Chithambo, M.L., 2003. The influence of annealing and partial bleaching on luminescence lifetimes in quartz. Radiat. Meas. 37, 467–472.

Chithambo, M.L., 2007a. The analysis of time-resolved optically stimulated luminescence. I: theoretical considerations. J. Phys. D Appl. Phys. 40, 1874–1879.

Chithambo, M.L., 2007b. The analysis of time-resolved optically stimulated luminescence. II: computer simulations and experimental results. J. Phys. D Appl. Phys. 40, 1880–1889.

Chithambo, M.L., 2018. An Introduction to time-resolved Optically Stimulated Luminescence (San Rafael. Morgan & Claypool Publishers.

Chithambo, M.L., Ogundare, F.O., Feathers, J., 2008. Principal and secondary luminescence lifetime components in annealed natural quartz. Radiat. Meas. 43, 1–4.

Chithambo, M.L., Ogundare, F.O., 2009. Luminescence lifetime components in quartz: influence of irradiation and annealing. Radiat. Meas. 44, 453–457.

Chithambo, M.L., 2011. A time-correlated photon counting system for measurement of pulsed optically stimulated luminescence. J. Lumin. 131, 92–98.

Chithambo, M.L., Sane, P., Tuomisto, F., 2011. Positron and luminescence lifetimes on annealed syntheitc quartz. Radiat. Meas. 46, 310–318.

Chithmabo, M.L., Ankjærgaard, C., Pagonis, V., 2016. Time-resolved luminescence from quartz: an overview of contemporary developments and applications. Physica B 481, 8–18.

Clark, R.J., Bailiff, I.K., Tooley, M.J., 1997. A preliminary study of time-resolved luminescence in some feldspars. Radiat. Meas. 27, 211–220.

Clark, R.J., Bailiff, I.K., 1998. Fast time-resolved luminescence emission spectroscopy in some feldspars. Radiat. Meas. 29, 553–560.

Deer, W.A., Howie, R.A., Zussman, J., 2013. An Introduction to rock-forming Minerals, third ed. Mineralogical Society, London, United Kingdom.

Del Río, I., Sawakuchi, A.O., Góes, A.M., Hollanda, M.H.B., Furukawa, L.Y., Porat, N., Jain, M., Mineli, T.D., de Assis Negri, F., 2021. Luminescence signals of quartz and feldspar as new methods for stratigraphic discrimination and provenance analysis of

siliciclastic successions: the case of the Parnaíba Basin (Brazil) of West Gondwana. Basin Res. 33, 2938–2959. https://doi.org/10.1111/bre.12590.
Denby, P.M., Bøtter-Jensen, Murray, A.S., Thomsen, K.J., Moska, P., 2006. Application of pulsed OSL to the separation of the luminescence components from a mixed quartz/feldspar sample. Radiat. Meas. 41, 774–779.
Dexter, D.L., Klick, C.C., Russel, G.A., 1955. Criterion for the occurrence of luminescence. Phys. Rev. 100, 603–605.
Finch, A.A., Klein, J., 1999. The causes and petrological significance of cathodoluminescence emissions from alkali feldspars. Contrib. Mineral. Petrol. 135, 234–243.
Galloway, R.B., 2002. Luminescence lifetimes in quartz: depenence on annealing temperature prior to beta irradiation. Radiat. Meas. 35, 67–77.
Gray, H.J., Jain, M., Sawakuchi, A.O., Mahan, S.A., Tucker, G.E., 2019. Luminescence as a sediment tracer and provenance tool. Rev. Geophys. 57, 987–1017. Doi: 10.129/2019RG000646.
Guerney, R.W., Mott, N.F., 1939. Luminescence in solids. Trans. Faraday Soc. 35, 69.
Guralnik, B., Ankjærgaard, C., Jain, M., Murray, A.S., Müller, A., Wälle, M., Lowick, S.E., Preusser, E.J., Wu, T.-S., Mathew, G., Herman, F., 2015. OSL-thermochronometry using bedrock quartz: a note of caution. Quat. Geochronol. 25, 37–48.
Harris, D.C., Bertolucci, M.D., 1989. Symmetry and Spectroscopy. an Introduction to Vibrational and Electronic Spectroscopy. Oxford Univeristy Press, Inc. Oxford, UK.
Herman, F., Rhodes, E.J., Braun, J., Heiniger, L., 2010. Uniform erosion rates and relief amplitude during glacial cycles in the Southern Alps of New Zealand, as revealed from OSL-thermochronology. Earth Planet Sci. Lett. 297, 183–189. https://doi.org/10.1016/j.epsl.2010.06.019.
Housecroft, C.E., Sharpe, A.G., 2018. Inorganic Chemistry, fifth ed. Pearson, Harlow, UK.
Hütt, G., Jaek, I., Tchonka, J., 1988. Optical Dating: K-feldspars optical response stimulation spectra. Quat. Sci. Rev. 7, 381–385.
Huntley, D.J., Godfrey-Smith, D.I., Haskell, E.H., 1991. Light–induced emission spectra from some quartz and feldspars. Nucl. Tracks Radiat. Meas. 18, 127–131.
Huntley, D.J., Short, M.A., Dunphy, K., 1996. Deep traps in quartz and their use for optical dating. Can. J. Phys. 74, 81–91.
Huntley, D.J., 2006. An explanation of the power-law decay of luminescence. J. Phys. Condens. Matter 18, 1359–1365.
Itoh, N., Stoneham, D., Stoneham, A.M., 2001. The predose effect in thermoluminescent dosimetry. J. Phys. Condens. Matter 13, 2201–2209.
Itoh, N., Stoneham, D., Stoneham, A.M., 2002. Ionic and electronic processes in quartz: mechanisms of thermoluminescence and optically stimulated luminescence. J. Appl. Phys. 92, 5036–5044. https://doi.org/10.1063/1.1510951.
Jain, M., Ankjægaard, C., 2010. Optically stimulated phosphoresence in quartz over the millisecond to second time scale: insights into the role of shallow traps in delaying luminescent recombination. J. Phys. Appl. Phys. 43, 255502. https://doi.org/10.1088/0022-3727/43/25/255502.
Jain, M., Buylaert, J.-P., Thomsen, K.J., Murray, A.S., 2015. Further investigations on non-fading in K-feldspar. Quat. Int. 362, 3–7. https://doi.org/10.1016/j.quaint.2014.11.018.
Kars, R.H., Wallinga, J., Cohen, K.M., 2008. A new approach towards anomalous fading correction for feldspar IRSL dating - tests on samples in field saturation. Radiat. Meas. 43, 786–790. https://doi.org/10.1016/j.radmeas.2008.01.021.
Kars, R.H., Poolton, N.R.J., Jain, M., Ankjægaard, C., Dorenbos, P., Wallinga, J., 2013. On the trap depth of the IR-sensitive trap in Na- and K-feldspar. Radiat. Meas. 59, 103–113. https://doi.org/10.1016/j.radmeas.2013.05.002.
King, G.E., Herman, F., Lambert, R., Valla, P.G., Guralnik, B., 2016. Multi-OSL-thermochronometry of feldspar. Quat. Geochronol. 33, 76–87. https://doi.org/10.1016/j.quageo.2016.01.004.
Klasens, M.A., 1946. Transfer of energy between centers in Zinc sulphide phospohors. Nature 158, 306–307.
Knoll, G.F., 2010. Radiation Detection and Measurement. John Wiley & Sons.
Kook, M., Kumar, R., Murray, A.S., Thomsen, K.J., Jain, M., 2018. Instrumentation for the non-destructive optical measurement of trapped electrons in feldspar. Radiat. Meas. 120, 247–252.
Krbetschek, M.R., Götze, J., Dietrich, A., Trautmann, T., 1997. Spectral information from minerals relevant for luminescence dating. Radiat. Meas. 5 (6), 695–748.
Kumar, R., Kook, M., Jain, M., 2021. Sediment dating using Infrared Photoluminescence. Quat. Geochronol. 62, 101147. https://doi.org/10.1016/j.quageo.2020.101147.
Kumar, R., Kook, M., Jain, M., 2020. Understanding metastable states in K-Na aluminosilicated using novel site-selective excitation-emission spectroscopy. J. Phys. Appl. Phys. 53, 465301.
Larsen, A., Greilich, S., Jain, M., Murray, A.S., 2009. Developing a numerical simulation for fading in feldspar. Radiat. Meas. 44, 467–471. https://doi.org/10.1016/j.radmeas.2009.03.035.
Li, B., Li, S.H., 2011. Luminescence dating of K-feldspar from sediments: a protocol without anomalous fading correction. Quat. Geochronol. 6, 468–479. https://doi.org/10.1016/j.quageo.2011.05.001.
Mandowski, A., Świątek, J., 1998. Thermoluminescence and trap assemblies—results of Monte Carlo calculations. Radiat. Meas. 29, 415–419. https://doi.org/10.1016/S1350-4487(98)00056-0.
Mandowski, A., 2004. Semi-localized transitions model for thermoluminescence. J. Phys. Appl. Phys. 38, 17–21. https://doi.org/10.1088/0022-3727/38/1/004.
Mandowski, A., 2008. Semi-localized transitions model-general formulation and classical limits. Radiat. Meas. 43, 199–202. https://doi.org/10.1016/j.radmeas.2007.10.009.
Martini, M., Paleari, A., Spinolo, G., Vedda, A., 1995. Role of $[AlO_4]^0$ centres in the 380-nm thermoluminescence of quartz. Phys. Rev. B 52, 138–142.
McKeever, S.W.S., 1994. Models for optical bleaching of thermoluminescence in sediments. Radiat. Meas. 23, 267–275.
Miessler, G.L., Fischer, P.J., Tarr, D.A., Inorganic Chemistry. fifth ed.. Pearson Education, Boston, USA.
Pagonis, V., Ankjægaard, C., Murray, A.S., Jain, M., Chen, R., Lawless, J., Greilich, S., 2010. Modelling the thermal quenching mechanism in quartz based on time-resolved optically stimulated luminescence. J. Lumin. 130, 902–909.
Pagonis, V., Morthekai, P., Singhvi, A.K., Thomas, J., Balaram, V., Kitis, G., Chen, R., 2012. Time-resolved infrared stimulated luminescence signals in feldspars: analysis based on exponential and stretched exponential functions. J. Lumin. 132, 2330–2340.
Pagonis, V., Chithambo, M.L., Chen, R., Chruscina, Fasoli, M., Li, S.H., Martini, M., Ramseyer, K., 2014. Thermal dependence of luminescence lifetimes and radioluminescence in quartz. J. Lumin. 145, 38–48.
Pagonis, V., Ankjægaard, C., Jain, M., Chithambo, M.L., 2016. Quantitative analysis of time-resolved infrared stimulated luminescence in feldspars. Physica B 497, 78–85. https://doi.org/10.1016/j.physb.2016.06.013.
Pagonis, V., Kulp, C., 2017. Monte Carlo simulations of tunneling phenomena and nearest neighbor hopping mechanism in feldspars. J. Lumin. 181, 114–120. https://doi.org/10.1016/j.jlumin.2016.09.014.
Pagonis, V., Friedrich, J., Discher, M., Müller-Kirschbaum, A., Schlosser, V., Kreutzer, S., Chen, R., Schmidt, C., 2019. Excited state luminescence signals from a random distribution of defects: a new Monte Carlo simulation approach for feldspar. J. Lumin. 207, 266–272. https://doi.org/10.1016/j.jlumin.2018.11.024.
Prasad, A.K., Lapp, T., Kook, M., Jain, M., 2016. Probing luminescence centres in Na rich feldspar. Radiat. Meas. 90, 292–297. https://doi.org/10.1016/j.radmeas.2016.02.033.
Prasad, A.K., Jain, M., 2018. Dynamics of the deep red Fe^{3+} photoluminescence in feldspar. J. Lumin. 196, 462–469. https://doi.org/10.1016/j.jlumin.2017.11.051.
Randall, J.T., Wilkins, M.H.F., 1945. Phosphorescence and electron traps 1. The study of trap distributions. Proc. Phys. Soc. Lond. 184, 366–389.
Riedesel, S., King, G.E., Prasad, A.K., Kumar, A., Finch, A.A., Jain, M., 2019. Optical determination of the width of the band-tail states, and the excited and ground state energies of the principal dosimetric trap in feldspar. Radiat. Meas. 125, 40–51. https://doi.org/10.1016/j.radmeas.2018.08.019.
Riedesel, S., Bell, A.M.T., Duller, G.A.T., Finch, A.A., Jain, M., King, G.E., Pearce, N.J., Roberts, H.M., 2021. Exploring sources of variation in thermoluminescence emissions and anomalous fading in alkali feldspars. Radiat. Meas. 141, 106541. https://doi.org/10.1016/j.radmeas.2021.106541.
Riedesel, S., Duller, G.A.T., Ankjærgaard, C., 2023. Time-resolved infrared stimulated luminescence of the blue and yellow-green emissions - insights into charge recombination in chemically and structurally different alkali feldspars. J. Lumin. 257, 119724. https://doi.org/10.1016/j.jlumin.2023.119724.
Rink, W.J., 1999. Quartz luminescence as a light-sensitive indicator of sediment transport in coastal processes. J. Coast Res. 15, 148–154.
Roskosch, J., Winsemann, J., Polom, U., Brandes, C., Tsukamoto, S., Weitkamp, A., Bartholomaeus, W., Henningsen, D., Frechen, M., 2015a. Luminescence dating of ice-marginal deposits in northern Germany: evidence for repeated glaciations during the Middle Pleistocene (MIS 12 to MIS 6). Boreas 44, 103e126.
Roskosch, J., Tsukamoto, S., Frechen, M., 2015b. Luminescence dating of fluvial deposits from the Weser valley, Germany. Geochronometria 42, 126e138.
Sanderson, D.C.W., Clark, R.J., 1994. Pulsed photostimulated luminescence of alkali feldspars. Radiat. Meas. 23, 633–639.
Sawakuchi, A.O., Jain, M., Mineli, T.D., Nogueira, L., Bertassoli, D.J., Häggi, C., Sawakuchi, H.O., Pupmin, F.N., Grohmann, C.H., Chiessi, C.M., Zabel, M., Mulitza, S., Mazoca, C.E.M., Cunha, D.F., 2018. Luminescence of quartz and feldspar fingerprints provenance and correlates with the source area denudation in the Amazon River basin. Earth Planet Sci. Lett. 492, 152–162. https://doi.org/10.1016/j.epsi.2018.04.006.
Scholonek, C., Augustsson, C., 2016. Can cathodoluminescence of feldspar be used as provenance indicator? Sediment. Geol. 336, 36–45. https://doi.org/10.1016/j.sedgeo.2015.11.005.
Schlag, E.W., Schneider, S., Fischer, S.F., 1971. Lifetimes in excited states. Annu. Rev. Phys. Chem. 22 (1), 465–526.
Schön, M., 1942. Zum Leuchtemechanismus der Kristallphosphore. Z. Phys. 119, 463–471 (in German).
Seitz, F., 1939. An interpretation of crystal luminescence. Trans. Faraday Soc. 35, 74.
Short, M.A., 2004. Determining the possible lattice sites of two unknown defects in orthoclase from the polarization effects in their optical transitions. J. Phys. Condens. Matter 16, 7405–7417.
Speit, B., Lehmann, G., 1982. Radiation defects in feldspars. Phys. Chem. Miner. 8, 77–82.
Sunta, C.M., David, M., 1982. Firing temperature of pottery from pre-dose sensitization of TL. PACT (Strasbg.) 6, 460–467.
Talele, S., King, J.T., 2021. Fast and robust two-dimensional inverse Laplace transformation of single-molecule fluorescence lifetime data. Biophys. J. 120, 4590–4599.
Tang, S.-L., Li, S.-H., 2015. Low temperature thermochronology using thermoluminescence signals from quartz. Radiat. Meas. 81, 92–97. https://doi.org/10.1016/j.radmeas.2015.04.011.
Tanski, N.M., Rittenour, T.M., Pavano, F., Pazzaglia, F., Mills, J., Corbett, L.B., Bierman, P., 2024. Quat. Geochronol. 84, 101613. https://doi.org/10.1016/j.quageo.2024.101613.
Thomsen, K.J., Jain, M., Murray, A.S., Denby, P.M., Roy, N., Bøtter-Jensen, L., 2008. Minimizing feldspar OSL contamination in quartz UV-OSL using pulsed blue stimulation. Radiat. Meas. 43, 752–757. https://doi.org/10.1016/j.radmeas.2008.01.020.

Tosi, A., Mora, A.D., Zappa, F., Gulinatti, A., Contini, D., Pifferi, A., Spinelli, L., Torricelli, A., Cubeddu, R., 2011. Fast-gated single-photon counting technique widens dynamic range and speeds up acquisition time in time-resolved measurements. Optic Express 19, 10735–10746.

Tsukamoto, S., Denby, P.M., Murray, A.S., Bøtter-Jensen, L., 2006. Time-resolved luminescence from feldspars: new insights into fading. Radiat. Meas. 41, 790–795.

Tsukamoto, et al., 2010. Charge recombination processes in minerals studied using optically stimulated luminescence and time-resolved exo-electrons. J. Phys. Appl. Phys. 43, 325502. https://doi.org/10.1088/0022-3727/43/32/325502.

Tsukamoto, S., Kondo, R., Lauer, T., Jain, M., 2017. Pulsed IRSL: a stable and fast bleaching luminescence signal from feldspar for dating Quaternary sediments. Quat. Geochronol. 41, 26–36. https://doi.org/10.1016/j.quageo.2017.05.004.

Watson, I.A., Aitken, M.J., 1985. Firing temperature analysis using the 100 °C peak of quartz. Nucl. Tracks 10, 517–520.

Williams, O.M., Spooner, N.A., 2025. Charge carrier release mechanisms underlying the emission of alkali feldspar infrared stimulated luminescence. Radiat. Meas. 181, 107362. https://doi.org/10.1016/j.radmeas.2024.107362.

Wintle, A.G., Murray, A.S., 1997. The relationship between quartz thermoluminescence, photo-transferred thermoluminescence, and optically stimulated luminescence. Radiat. Meas. 27, 611–624.

Zhang, J., Tsukamoto, S., Long, H., 2023. Testing the potential of pulsed post-IR IRSL dating on Chinese loess deposits. Quat. Geochronol. 78, 101469. https://doi.org/10.1016/j.quageo.2023.101469.

Zimmerman, J., 1971. The radiation-induced increase of the 100 C thermoluminescence sensitivity of fired quartz. J. Phys. C Solid State Phys. 4, 3265–3276.